Development of the Coastal Storm Modeling System (CoSMoS) for predicting the impact of storms on high-energy, active-margin coasts

Citation	Barnard, P. L., van Ormondt, M., Erikson, L. H., Eshleman, J., Hapke, C., Ruggiero, P., ... & Foxgrover, A. C. (2014). Development of the Coastal Storm Modeling System (CoSMoS) for predicting the impact of storms on high-energy, active-margin coasts. Natural Hazards, 74(2), 1095-1125. doi:10.1007/s11069-014-1236-y
DOI	10.1007/s11069-014-1236-y
Publisher	Springer
Version	Version of Record
Terms of Use	http://cdss.library.oregonstate.edu/sa-termsofuse

Nat Hazards (2014) 74:1095–1125
DOI 10.1007/s11069-014-1236-y

ORIGINAL PAPER

Development of the Coastal Storm Modeling System (CoSMoS) for predicting the impact of storms on high-energy, active-margin coasts

Patrick L. Barnard · Maarten van Ormondt · Li H. Erikson · Jodi Eshleman · Cheryl Hapke · Peter Ruggiero · Peter N. Adams · Amy C. Foxgrover

Received: 28 January 2014 / Accepted: 11 May 2014 / Published online: 21 May 2014

Abstract The Coastal Storm Modeling System (CoSMoS) applies a predominantly deterministic framework to make detailed predictions (meter scale) of storm-induced coastal flooding, erosion, and cliff failures over large geographic scales (100s of kilometers). CoSMoS was developed for hindcast studies, operational applications (i.e., nowcasts and multiday forecasts), and future climate scenarios (i.e., sea-level rise + storms) to provide emergency responders and coastal planners with critical storm hazards information that may be used to increase public safety, mitigate physical damages, and more effectively manage and allocate resources within complex coastal settings. The prototype system, developed for the California coast, uses the global WAVEWATCH III wave model, the TOPEX/Poseidon satellite altimetry-based global tide model, and atmospheric-forcing data from either the US National Weather Service (operational mode) or Global Climate Models (future climate mode), to determine regional wave and water-level boundary conditions. These physical processes are dynamically downscaled using a series of nested

P. L. Barnard (✉) · L. H. Erikson · A. C. Foxgrover
Pacific Coastal and Marine Science Center, United States Geological Survey, 400 Natural Bridges Drive, Santa Cruz, CA 95060, USA
e-mail: pbarnard@usgs.gov

M. van Ormondt
Deltares-Delft Hydraulics, P.O. Box 177, 2600 MH Delft, The Netherlands

J. Eshleman
Geologic Resources Division, Natural Resource Program Center, National Park Service, Lakewood, CO, USA

C. Hapke
Coastal and Marine Geology Program, United States Geological Survey, St. Petersburg, FL, USA

P. Ruggiero
Department of Geosciences, Oregon State University, 104 Wilkinson Hall, Corvallis, OR, USA

P. N. Adams
Department of Geological Sciences, University of Florida, 241 Williamson Hall, Gainesville, FL, USA

Delft3D-WAVE (SWAN) and Delft3D-FLOW (FLOW) models and linked at the coast to tightly spaced XBeach (eXtreme Beach) cross-shore profile models and a Bayesian probabilistic cliff failure model. Hindcast testing demonstrates that, despite uncertainties in preexisting beach morphology over the ~500 km alongshore extent of the pilot study area, CoSMoS effectively identifies discrete sections of the coast (100s of meters) that are vulnerable to coastal hazards under a range of current and future oceanographic forcing conditions, and is therefore an effective tool for operational and future climate scenario planning.

Keywords Modeling · Storms · Inundation · Erosion · Cliff · Beach · Hazards

1 Introduction

Coastal communities throughout the world will face increasing hazard risks as climate change drives sea-level rise (SLR) and possible increased storminess, resulting in inundation, flooding, and erosion that could force millions of people to migrate from the coast at a cost of up to $1 trillion during the twenty-first century (e.g., Nichols 2004; Hinkel et al. 2013). The ability to accurately predict the impact of storms on the coastal environment will be critical for coastal planners and emergency response managers to mitigate the loss of life and property damage during severe storm events.

Research on ice sheet dynamics (Pfeffer et al. 2008) and semi-empirical approaches relating global temperature to SLR (e.g., Vermeer and Rahmstorf 2009) has projected a range of global SLR from 0.75 to 2 m by 2100. The National Research Council (2012) is projecting ~1 m of SLR along the US West Coast by 2100 (range 0.1–1.7 m), with significant variability latitudinally primarily due to tectonic setting, the gravitational effects of melting ice sheets (i.e., SLR fingerprinting), and ocean and atmospheric circulation patterns. However, the impact of SLR is only one aspect of climate change and variability that must be considered. When assessing coastal hazard vulnerability, seasonal and storm-induced dynamic coastal water levels must also be included, particularly on the US West Coast and other wave- and storm-dominated settings worldwide.

Decadal and interannual climate fluctuations have a significant impact on regional ocean circulation and weather patterns (e.g., Pacific Decadal Oscillation and El Niño Southern Oscillation) as well as pronounced seasonal and storm effects that ultimately drive coastal flooding and erosion by producing elevated water levels and powerful waves. For example, along the US West Coast, seasonally averaged coastal water levels can be elevated up to 0.5 m during El Niño periods (Allan and Komar 2006) and coastal storm surges can reach 1.4 m (Allan et al. 2011). Wave setup can theoretically approach 2 m during extreme events (Guza and Thornton 1981), with wave run-up elevating coastal water levels up to several additional meters (Stockdon et al. 2006; CDIP 2013). Increases in wave heights over the last several decades have been documented along portions of the US West Coast (e.g., Allan and Komar 2006; Menendez et al. 2008; Ruggiero et al. 2010; Gemmrich et al. 2011; Young et al. 2011), suggesting that the rate of increase in wave-driven water levels may be outpacing the rate of SLR in certain areas for at least several more decades (Ruggiero 2013). The use of Global Climate Models (GCMs) to determine the future wave climate suggests a nonlinear evolution as the projected poleward migration of storm tracks may result in local changes in wave height, period, and direction compared

to the historical record (Hemer et al. 2013). Santoso et al. (2013) project a doubling of El Niño events in the future, which often results in significant coastal damage along the US West Coast due to the hazardous combination of anomalously high winter water levels and wave energy, along with more southerly wave approaches (Barnard et al. 2011). Even if the wave climate remains relatively stationary, storm-related coastal water levels will be more frequent and higher in the future due to SLR, resulting in greater risk of coastal flooding and severe erosion compared to the present. Therefore, regardless of the precise nature of twenty-first century climate change, any robust projections of coastal hazards must include both SLR and storms.

Few attempts have been made to develop comprehensive, deterministic models that scale down from ocean basin to beach scale, including coupled ocean–atmospheric forcing. The NOAA Coastal Services Center's Sea-Level Rise and Coastal Flooding Impacts Viewer (NOAA 2013b) projects coastal flooding associated with climate change, but is based on SLR and astronomical tides only. The Federal Emergency Management Agency (FEMA) introduced the Coastal Hazard Analysis Modeling Program (CHAMP) to perform coastal hazards assessments along cross-shore transects, but is not designed for West Coast applications and is only available as an offline tool (FEMA 2007). The Morphological Impacts and COastal Risks induced by Extreme storm events (MICORE) program for the European Union (e.g., van Dongeren et al. 2009) is following a similar model framework to CoSMoS, but the primary objective is the development of an operational warning system. Warner et al. (2010) developed the Coupled Ocean–Atmosphere–Wave–Sediment Transport (COAWST) Modeling System for the US East Coast, primarily to assess hurricane impacts. Their work followed a series of other coupled approaches that focused exclusively on hurricane impacts (e.g., Bender and Ginis 2000; Bender et al. 2007; Chen et al. 2007).

The nearshore model is a key component for any coastal hazards modeling system, as it ultimately predicts coastal wave heights and water levels that supply information to the hazard assessments. A process-based approach that utilizes wave group forcing (e.g., XBeach) is essential for effectively modeling high-energy, dissipative coastal settings such as the US West Coast, where wave setup and infragravity swash are two of the most important physical processes that must be considered during storms, with surge typically playing only a secondary role. Several studies have compared XBeach model results with the measurements of beach and dune response to storm events. Roelvink et al. (2009) discussed numerous test cases used for validation that compare model results with analytical, laboratory, and field data sets. McCall et al. (2010) applied XBeach at Santa Rosa Island (Florida, USA) to predict overwash and barrier island response to hurricane forcing in a two-dimensional domain. As a component of the European project MICORE, investigators compared the results of beach profile hindcasting using XBeach as well as other 1D off-the-shelf models and showed that XBeach shows skill in predicting the coastal profile, although it generally overpredicts erosion around the mean water line and deposition on the lower beach face (Van Dongeren et al. 2009). Splinter and Palmsten (2012) demonstrated that XBeach adequately reproduced dune retreat (within 7–11 % of observed change) during a storm along the Gold Coast of Australia, and unlike more simple parametric models that can only erode landward of the initial dune toe and above the initial beach slope, XBeach is capable of eroding the entire active profile. However, they cautioned that results were sensitive to tuning parameters and may require site-specific calibration.

There has been less focus on regional hazards modeling on the US West Coast relative to studies of hurricane impacts that affect the Gulf of Mexico and East Coasts. However,

the economic and societal impact of severe winter storms on the west coast can be substantial. For example, storms that occurred during the 1982–1983 El Niño winter resulted in 36 casualties and over $1.2 billion dollars in damage to the State of California (NWS 2012), including the destruction of numerous piers and other coastal infrastructure. Nevertheless, there exists no real-time warning system or process-based coastal vulnerability tool to prepare US West Coast communities for the impact of current or future storms to mitigate hazards. This paper introduces a new, process-based modeling system that has been designed to assess the physical impacts (e.g., flooding, beach erosion, and cliff failures) of severe storms both operationally and based on future SLR/climate change scenarios. Although the modeling system was initially developed for use on the high-wave-energy environment of the US West Coast, CoSMoS is not empirically based and can be utilized on sandy and/or cliff-backed coasts throughout the world.

The paper is structured as follows: Sect. 2 describes the general model framework; Sect. 3 describes in detail a case study application utilizing both operational and climate change aspects in Southern California (i.e., CoSMoS 1.0), including a validation of various model components; Sect. 4 briefly summarizes a case study application for future climate scenarios in North-central California (i.e., CoSMoS 2.0) with full details to be made available in a future publication; Sect. 5 discusses future work and conclusions.

2 Model framework

A conceptual overview of the CoSMoS framework is given in Fig. 1. Boundary conditions for the regional Delft3D hydrodynamic and wave models that extend from deep water to the coastal study area and for ~10s–100s of km alongshore are determined by output from the global (NWW3) and nested Eastern North Pacific (ENP) grids of the NOAA WAVEWATCH III model (Tolman 1997, 2009; NOAA 2011), the global TOPEX/Poseidon tide model, atmospheric pressure and wind data, and bathymetric data sets. The required inputs are swell, seas, wind, atmospheric pressure, tidal constituents, and bathymetry. After a series of nesting procedures, the regional models provide boundary conditions at the offshore end of the local high-resolution Delft3D and cross-shore XBeach profile models. XBeach cross-shore profiles are co-located with the MOnitoring and Prediction (MOP) points established by the Scripps Institution of Oceanography's Coastal Data Information Program (Coastal Data Information Program (CDIP) 2013). The XBeach models extend from the 10-m (CoSMoS 1.0) or 15-m (CoSMoS 2.0) depth contour to an inland elevation >+10 m, with spacing every 100–200 m alongshore. The XBeach models provide the critical interface where waves and water levels are translated across the surf zone and onto the beach in high-wave-energy open-coast settings.

2.1 Boundary conditions

2.1.1 Global wave model

For operational applications, the NOAA regional ENP model provides 2D spectral boundary input for the regional Delft3D-WAVE model (i.e., SWAN). The ENP model itself is nested in the global NWW3 model through a one-way nesting procedure. The NWW3 and ENP model simulations are executed within the CoSMoS system. The NWS National Center for Environmental Prediction (NCEP) publishes results from its (nearly) identical operational NWW3 and ENP models twice-daily online, but CoSMoS requires

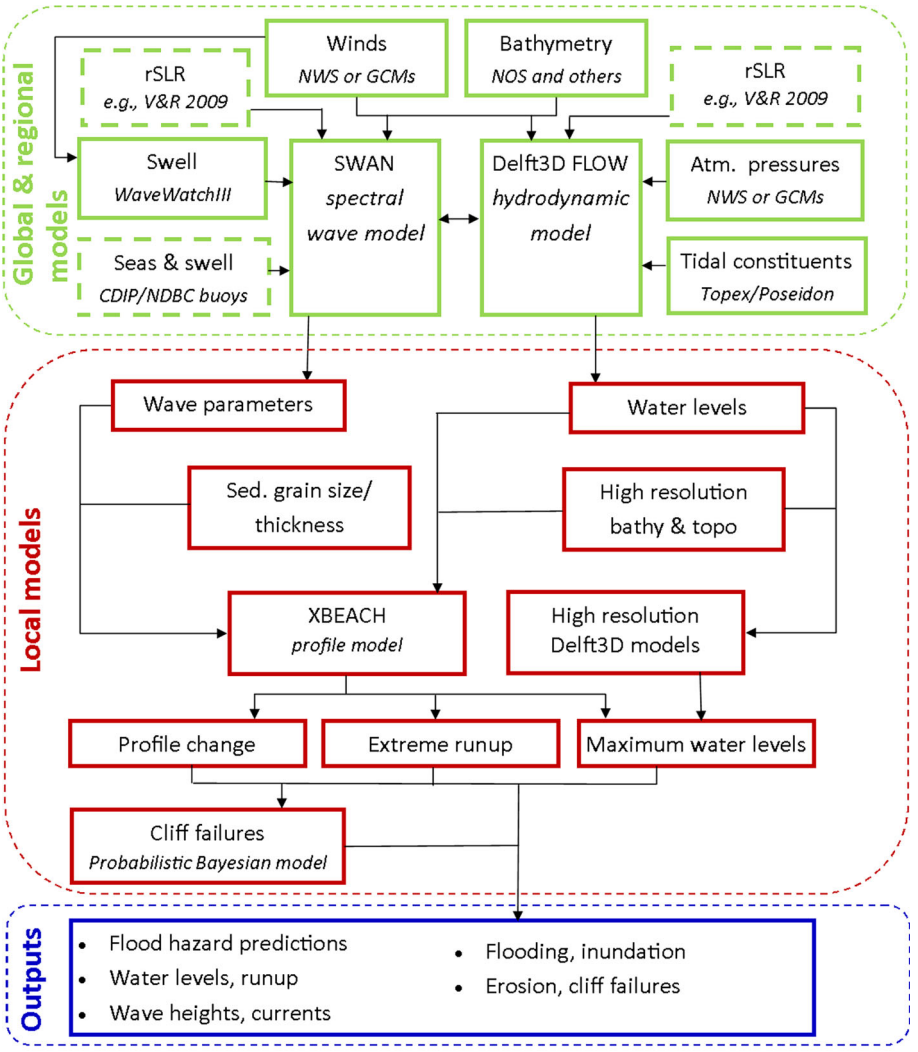

Abbreviations: GCMs: Global Climate Models; rSLR: relative sea level rise; NOS:National Ocean Service; NWS: National Weather Service ; CDIP: Coastal Data Information Program; NDBC: National Data Buoy Center; V&R: Vermeer and Rahmstorf

Fig. 1 CoSMoS model framework. The flowchart depicts interactions among the global, regional, and local models; boundary data used to drive the models; and model outputs. Dashed boxes indicate the use of these parameters when applicable (e.g., the rSLR is only used for the simulation of projected conditions, not for operational mode). Communication between the models and formatting of input/output data are controlled with a suite of MATLAB® scripts. Relatively little manual file manipulation is required

high-resolution 2D spectral output along the open boundaries of the Delft3D model, which is not provided in the NCEP products.

For future climate scenario applications, a suite of Global Climate Model (GCM)-derived wind fields from the Coupled Model Intercomparison Project Phase 5 (CMIP5 2011) drive the global NWW3 and ENP models to determine the wave climate for the

twenty-first century off the continental shelf in deep water. These deepwater wave statistics serve as boundary conditions for the future climate scenarios that then drive the open boundaries of the Delft3D-WAVE models.

2.1.2 Tidal forcing

Tidal boundary conditions for the regional-scale tide model (Delft3D-FLOW) are obtained from the Oregon State University (OSU) TOPEX/Poseidon global tide database (Egbert et al. 1994). The Southern California model is forced with weakly reflective Riemann boundaries (Verboom and Slob 1984). The Riemann invariants were derived from 13 harmonic constituents of sea surface elevation and tidal currents in the TPXO7.2 database. Similarly, the open boundaries for the North-central California model were also derived from tidal constituents of the TOPEX/Poseidon database. Constituent amplitudes and phases were used as initial estimates and then adjusted so that differences between observed and modeled water levels within the model domain were minimized [see (Elias and Hansen 2013) for further details].

2.1.3 Atmospheric forcing

Atmospheric forcing in CoSMoS for operational applications is provided by NCEP products. Wind data (10 m above sea surface) from the Global Forecasting System (GFS) are applied to force the two WAVEWATCH III models. The regional Delft3D models are forced with data from the North American Mesoscale Forecasting System (NAM). Winds from NAM are used for wave generation on the regional scale (in Delft3D-WAVE) and to compute local wind setup near the coast (in Delft3D-FLOW). The regional models also take into account the effects of spatially and temporally varying atmospheric pressure within the model domains. Additionally, time-varying water levels in response to large-scale (Pacific basin) circulation patterns are obtained from the HYbrid Coordinate Ocean Model (HYCOM, http://hycom.org/hycom/) database and applied along the open boundaries of the Delft3D-FLOW and Delft3D-SWAN models. For future scenarios, wind and pressure fields are derived from the output of GCMs.

2.1.4 Digital elevation models

For each coastal study site, seamless digital elevation models (DEM) at $\sim$2–3 m resolution are constructed to integrate the most recent, high-resolution data sets available (e.g., light detection and ranging (Lidar) topography, multibeam and single-beam sonar bathymetry, and Interferometric Synthetic Aperture Radar (IfSAR) topography) into a continuous surface from at least the 20 m isobath to the 20 m elevation contour (Fig. 2). The DEMs are constructed to define the shape of nearshore, beach, and cliff surfaces as accurately as possible, typically utilizing dozens of bathymetric and topographic data sets. Based on this surface, elevation data are extracted as an initial boundary condition for local high-resolution Delft3D models (e.g., nearshore and protected embayments) and XBeach models. For more information on DEM construction methods, see Barnard and Hoover (2010) and Foxgrover and Barnard (2012); the data are available at http://topotools.cr.usgs.gov/topobathy_viewer/.

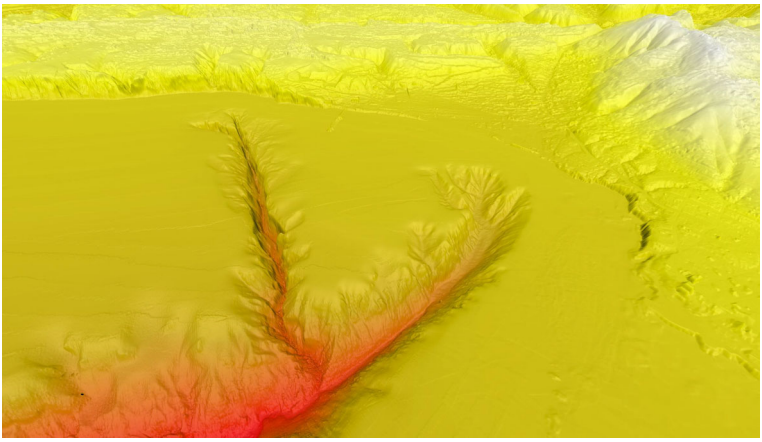

Fig. 2 Perspective view of a seamless DEM in the La Jolla region, constructed primarily from topographic Lidar and multibeam bathymetry data sets, featuring submarine canyon lobes and coastal bluffs (from Barnard and Hoover 2010)

2.2 Regional/local wave and tide models

A framework of coupled model 2D (depth-averaged) grids are built in the Delft3D-FLOW and Delft3D-WAVE models (Lesser et al. 2004; Delft Hydraulics 2007) with sufficient resolution to resolve wave conditions and stationary water levels at the offshore boundary of the XBeach models. SWAN version 4.72 forms the computational core of Delft3D-WAVE. This framework allows (1) the flexible coupling of large-scale regional models and high-resolution models at key coastal locations, and (2) the exchange of input and output data with other models used in this modeling system (e.g., XBeach). The regional model grid resolution increases toward the coastline. The cross-shore grid spacing along the 10-m depth contour is approximately 100 m. The large-scale model is forced with tidal constituents at the open boundary and wave action through a link to the WAVEWATCH III model. The primary atmospheric-forcing parameters, surface winds and atmospheric pressure, are obtained from the National Weather Service real-time forecasts (NWS 2013). Bathymetry data outside of the DEM footprint (>20 m depth) are obtained from regional, relatively coarse DEMs with typical resolutions ranging from 10 to 90 m. Water-level output and wave data from the regional models are 2-way coupled with a series of higher-resolution Delft3D models at key coastal sites in CoSMoS 2.0, such as harbors, inlets, river mouths, piers, and vulnerable beaches, where greater detail in wave forcing and hydrodynamics is desirable to better resolve local flooding vulnerability.

2.3 Cross-shore profile model

XBeach (Roelvink et al. 2008, 2009) is applied in one dimension to predict the cross-shore profile evolution, wave setup, extreme run-up, and maximum total water level along each transect. XBeach was run in profile mode (as opposed to 2D mode) to save computational time ($\sim$100-fold) and under the assumption that cross-shore processes (e.g., wave setup and run-up) dominate total water levels and coastal flooding extents along US West Coast

beaches due to the large, long-period nature of storm waves that refract appreciably on the inner shelf and break at angles often approaching shore normal.

The version described in Roelvink et al. (2009) has been modified for this analysis to use Snell's Law for wave direction and optimized for computational speed. The model domain extends from the 10- or 15-m-depth contour to at least the 10-m elevation contour, and the bathymetry input was extracted from the high-resolution coastal DEM. Sediment in the cliff sections (greater than 30° slope) is considered to be immobile in XBeach, and cliff failure is modeled using a probabilistic approach described in Sect. 2.6.1. The XBeach model was not calibrated with field data in CoSMoS 1.0, as survey data that captures beach profile response to individual storms is very limited within the study area. The goal for CoSMoS is to consider variations in coastal hazards at a regional scale without requiring detailed calibration at specific sites. The model was applied with standard parameters throughout the study area. In CoSMoS 2.0, field data were used to adjust XBeach parameter settings to better represent sediment transport. Grid spacing ranged from 30 m offshore to a constant 5 m resolution shoreward of 2.5 m water depth. Sediment size (0.25 and 0.28 mm in version 1.0 and 2.0, respectively) and availability (2 m thickness) along the profiles were held constant. The model was forced with water-level data and 2D SWAN spectra that were output from the regional Delft3D-FLOW/WAVE models at the outer boundary of each profile model. The time series of run-up elevation predicted by XBeach was used to develop input for the probabilistic cliff failure model, and the modeled water levels were used to estimate areas of flooding and inundation. The final modeled profile was compared to input bathymetry to estimate statistics related to shoreline change and profile evolution for the modeled storm.

2.4 Flood extent determination

Flood extents are determined in two ways: (1) from maximum wave run-up (CoSMoS 1.0) or setup (CoSMoS 2.0) calculated with the XBeach cross-shore model on the open coast, and (2) from the landward-most wet grid cell in the high-resolution Delft3D grids in protected embayments (e.g., in harbors and estuaries, CoSMoS 2.0 only). Because the XBeach profile model generates intermittent water-level predictions ($\sim$100–200 m spacing) along coast, an additional step is needed to generate a continuous flood map. To do this, the topographic elevation of the flood level is extended landward along the entire length of the XBeach profile (extending inland to an elevation of greater than 10 m) and the water elevation between profiles interpolated using a Triangulated Irregular Network (TIN). This water elevation TIN is converted to a raster and differenced from the high-resolution DEM to isolate areas where the water level exceeds the elevation of the topography, indicating flooding. Only flood cells that are adjacent to cells connected to the ocean are retained to eliminate isolated low-lying areas that are below the flood elevation, but not hydraulically connected to the ocean. In addition to flooding extent, estimates of flood depth and uncertainties in flood extent stemming from inaccuracies in DEM elevations and/or model results are generated with this technique.

The maximum landward extent of the swash lens calculated with the XBeach model was used as the topographic elevation from which the continuous flood maps were generated in CoSMoS 1.0. Because the swash lens is often thin and contains a limited volume of seawater, this approach overestimated the flood extents in some areas. Therefore, an estimate of the wave setup was used as the "flood elevation" in CoSMoS 2.0 along the exposed outer coast. Wave setup was calculated from low-pass filtered (Butterworth, frequency cutoff = 0.0167 Hz) time series of water levels extracted from the 0.5 m

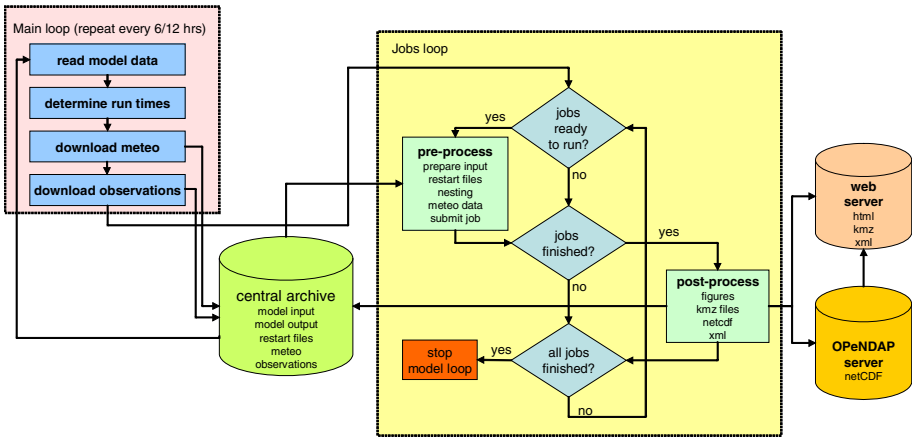

Fig. 3 Conceptual workflow of the CoSMoS model. For nonoperational model simulations, input data are supplied from other sources and outputs are not uploaded to the Web or OPeNDAP servers

isobath. The maximum water elevation attained at the 0.5 m isobath is then extrapolated to intersect with the beach profile and effectively represents standing water of at least 1 min. The wave setup approach for estimating coastal flooding is a better indicator of coastal regions that are subject to persistent, potentially damaging flooding during a given storm, as opposed to the more conservative wave run-up approach, which indicates less frequent, shallower flooding.

2.5 Computational framework

The models within CoSMoS are linked using a series of MATLAB® scripts that were developed to manipulate input/output data and run the models (Fig. 3). Two process loops are continuously executed at set intervals:

- The main loop: This loop is executed every 6 or 12 h when making operational forecasts. For future scenario computations, it is executed only once. The main loop reads meta-information (in XML format) of each model and determines the start and stop times, taking into account the required spin-up times for the different models. Next, it downloads the required meteorological data from the NCEP OPeNDAP servers, as well as real-time observations from the National Data Buoy Center (NOAA 2013a) and National Ocean Service tide stations (NOAA 2013c) and stores these in a central database. The real-time data are only used to generate figures for model-data comparisons.
- The job loop: This loop is executed every 10 s. Within the job loop, the CoSMoS system first checks whether model simulations are ready to run. The main requirement for a model to be executed is that the overall model simulation from which it gets its boundary conditions has finished and has been processed. When a model is ready to run, the system prepares its input using the data stored in the central archive. This step includes the nesting procedure (for both water levels and 2D wave spectra), copying restart files, and converting meteorological data into the proper format. Once all the model input has been prepared, the simulation is submitted to be run on a Linux cluster. In each job loop, the system checks whether any simulations have finished running. If

Table 1 Range and means of data variables incorporated into the Bayesian network for cliff retreat

Model parameter	Max.	Min.	Mean
Santa Barbara ($n = 156$)			
Long-term retreat rate (m/year)	−0.8	−0.01	−0.2
Cliff slope (°)	63.6	14.9	40.5
Cliff height (m)	50.0	6.2	24.5
Geologic ranking	2	1	–
Impact minutes	1,782	0	26.4

this is the case, they go through a number of post-processing steps. The model output is first converted into the Network Common Data Form (NetCDF) format and stored on an OPeNDAP server. Next, a series of figures, comparing model results and observed data, is made, and a number of kmz files containing model output are generated. For each XBeach model, potential hazard data, such as inundation, coastal erosion, and shoreline change, are extracted from the model results and stored in an XML file. The figures, kmz files, and potential hazard XML files are copied to the CoSMoS Web server. A website with a Google Earth interface (http://cosmos.deltares.nl/SoCalCoastalHazards/index.html) displays the model results in an interactive way, highlighting locations where hazards are expected. The last step in the job loop is to check whether all simulations have finished running. If this is the case, execution of the job loop is stopped. Otherwise, the entire jobs loop is executed again after 10s.

2.6 Pilot modules

2.6.1 Cliff failure—Bayesian model development

In this portion of the CoSMoS modeling system, a multi-parameter Bayesian network is integrated to investigate correlations between key variables that control and influence cliff response to storms. The network uses Bayesian statistical methods to estimate event probabilities using existing observations (Hapke and Plant 2010). Input parameters include height and slope of the cliff at each XBeach transect, a descriptor of material strength based on the dominant cliff-forming lithology (geologic ranking, Table 1) and long-term cliff erosion rates representing prior behavior (Table 1). The model is initiated using wave impact minutes generated using the time series of run-up estimates from XBeach to forecast areas with the highest probability of cliff-top retreat. The selected parameters were chosen as being critical for forecasting retreat and were shown to all contribute significantly to the resulting forecast in Hapke and Plant (2010).

The model data were generated for transects coincident with the XBeach models for a pilot study spanning a 16-km stretch of coast in Santa Barbara. This portion of the Southern California coast was chosen for the simulated storm cliff response because of the variable cliff morphology (cliff height and slope) and the variation in amount of cliff-top development and engineering structures. One goal of the analysis is to assess whether the forecasting capabilities of the model are influenced by development or human modifications within a system. Of the 362 XBeach models in the Santa Barbara area, only 156 are coincident with cliffs and in areas where input criteria were available.

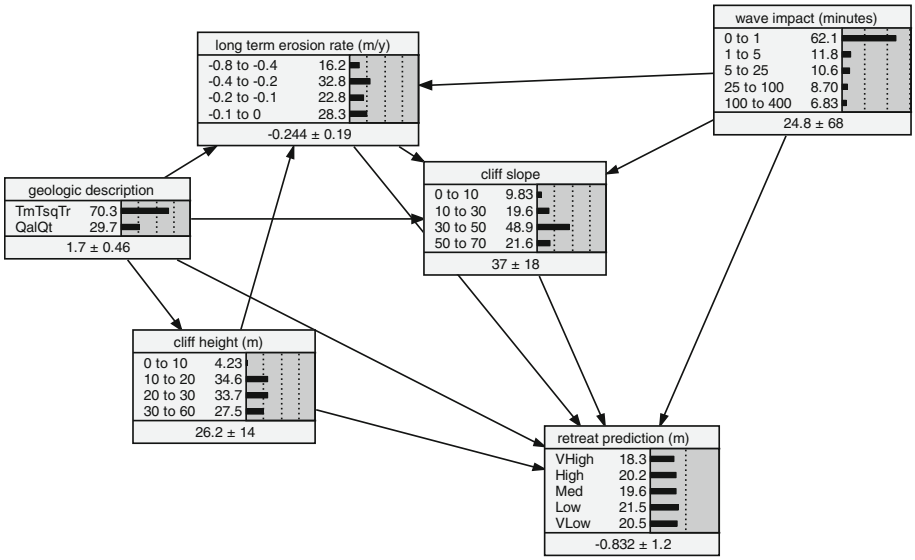

Fig. 4 Bayes network used in the cliff retreat prediction model. *Arrows* are vectors indicating the inferred causal relationship between parameters

The cliff slope, height, basal elevation, top edge position, and top elevation (Table 1) were each extracted from a 2005 Lidar survey that was also one of the primary data sets in the coastal DEM (see Sect. 2.1.4). The top edge of the cliff was interpreted and digitized from the Lidar data using methods developed by Hapke and Reid (2007), and the elevations of the cliff top and base were determined from the grid cell elevation value where each transect intersects the line defining the cliff top and base.

Long-term retreat rates are input as a descriptor of the prior behavior of the cliffs. The rates are ~70-year historic rates from Hapke and Reid (2007) and ranged from −0.01 to −0.8 m/year (Table 1). A simplified geologic descriptor, intended to represent a relative "erodibility ranking," was assigned at each transect by identifying the primary cliff-forming geologic unit. Geologic units were initially determined from a digital statewide coastal geology GIS database (Griggs unpub. data) and subsequently refined using available geologic maps of the area (Minor et al. 2002). The geologic units in the study area were grouped into two relative erodibility categories: (1) quaternary shallow marine and alluvial deposits (Qal and Qt in Fig. 4); and (2) various Pliocene and Miocene-age shales and mudstones of the Monterey Formation, and the Sisquoc Formation, a lower Pliocene and upper Miocene mudstone, shale, and conglomerate (Tm, Tsq and Tr in Fig. 4).

The parameters are incorporated into a Bayesian network (Fig. 4), similar to that developed and verified by Hapke and Plant (2010). For each parameter in the network, the data were binned (Table 2) to provide as wide a distribution as possible. Bin widths, where applicable (i.e., long-term behavior), also attempt to represent uncertainty limits of the data. The Bayesian network incorporates conditional relationships into the model. This is indicated by unidirectionally linked parameters (i.e., geology and cliff slope) that imply a causal relationship in the direction indicated by the vectors (Fig. 4).

Table 2 Bin boundary values for cliff retreat model parameters

Model parameter	Bin boundary values
Long-term retreat rate	0 −0.1 −0.2 −0.4 −0.8
Cliff slope	0 10 30 50 70
Cliff height	0 10 20 30 60
Geologic ranking	1 2
Impact minutes	0 1 5 25 100 2,000
Storm retreat	0 −0.1 −0.3 −0.5 −1.0 −5.0

2.6.2 Longshore transport gradients

While cross-shore sediment transport within CoSMoS is simulated by XBeach and is believed to generally dominate the sediment transport signal during storm events on US West Coast beaches, here we present a pilot module for identifying erosion due to variability in alongshore transport gradients. Coastal erosion and shoreline retreat occur when there is a decrease in littoral zone sediment at a site, which is a manifestation of a positive gradient in longshore sediment transport rate. Calculations of longshore sediment transport gradients were made by applying the Komar and Inman (1970) or CERC (1984) formula to wave conditions at each XBeach transect and differencing the transport rates alongshore. The volumetric sediment transport rate is given by

$$Q_l = K\frac{E\mathrm{Cn}\cos\alpha\sin\alpha}{g(\rho_s-\rho_w)(1-\eta)} \tag{1}$$

where K is a constant (calibrated to 0.8 from specific sites along the Southern California coast), g is gravitational acceleration, ρ_s and ρ_w are sediment and water density, respectively, and η is porosity of the subaqueous beach. Wave-breaking conditions for E, the wave energy density C, wave celerity n (1/2 for shallow water), and α angle of incidence are typically used in this formula. In this study, however, we use the wave conditions at the outer boundary of the XBeach models in 10 m of water depth for the calculation of longshore sediment transport (LST) rate. It should be noted that Eq. (1) assumes a transport-limited scenario; hence, it provides an estimate of longshore sediment transport potential. To obtain the volumetric change in beach sediment volume, also referred to as the divergence of drift, within a particular reach of coast between any two XBeach transects, the first spatial derivative of Q_l is evaluated. Results of the application of this analysis over a 10 km reach for the ARkStorm scenario described below are presented in the results section.

3 CoSMoS 1.0: Case study for Southern California

3.1 Study area and model setup

CoSMoS was initially developed and tested for the Southern California Bight (CoSMoS 1.0), which extends 470 km from Pt. Conception, California (USA), south to the Mexican border (Fig. 5). The region includes microtidal basins but has few significant inlets or narrow straits that would focus tidal currents in the nearshore. The coastline is highly variable in terms of its orientation (west to south facing), morphology (rocky to wide, flat

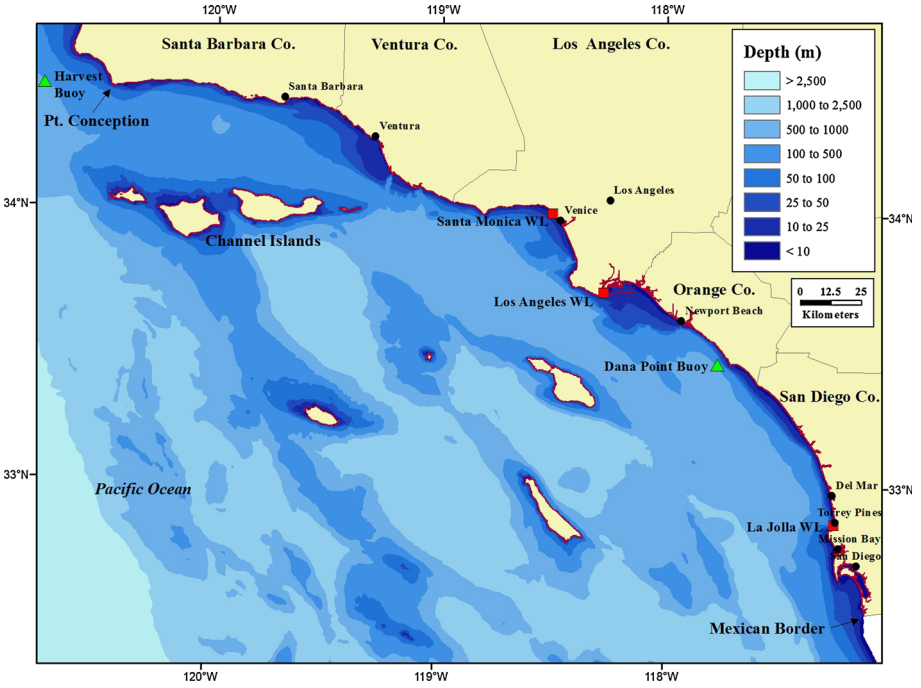

Fig. 5 Overview of the study area for CoSMoS 1.0 in Southern California, with locations of wave buoys (*triangles*) and water-level stations (*squares*) described in the text (modified from Barnard et al. 2009)

beaches), structures (seawalls, jetties, groins, breakwaters, etc.), exposure (open to significant island sheltering), and backbeach development (rural coast to urban beach front). The continental shelf is narrow (<20 km), so storm surge during even the largest winter storms is ≪1 m throughout California (e.g., Bromirski et al. 2003; Cayan et al. 2008), and therefore, extreme coastal flooding is usually caused by waves via setup and swash (i.e., run-up).

Deepwater swell is primarily from the west and northwest, but long-period southern swell can be important during the summer months and during El Niño years (O'Reilly 1993; Adams et al. 2008). Wave energy is highly seasonal and episodic, with winter storms capable of significantly eroding local beaches (Shepard 1950). To address nearshore wave variability adequately, Southern California wave modeling requires a high spatial resolution bathymetry grid in water depths less than 300 m and high-resolution directional wave spectra at the model-domain boundaries (O'Reilly and Guza 1993; O'Reilly et al. 1993). DEMs for the entire Southern California coastal zone were developed at 3-m horizontal resolution using more than 40 bathymetric and topographic data sets (Barnard and Hoover 2010). The set of regional models consists of the large-scale Southern California model, and three nested regional models of the Santa Barbara Channel, Los Angeles/Orange County, and San Diego coastlines (Fig. 6).

3.2 Storm scenarios

A team of atmospheric scientists with expertise in West Coast storms devised a stitching method to adapt information from two powerful West Coast storms that occurred in 1969

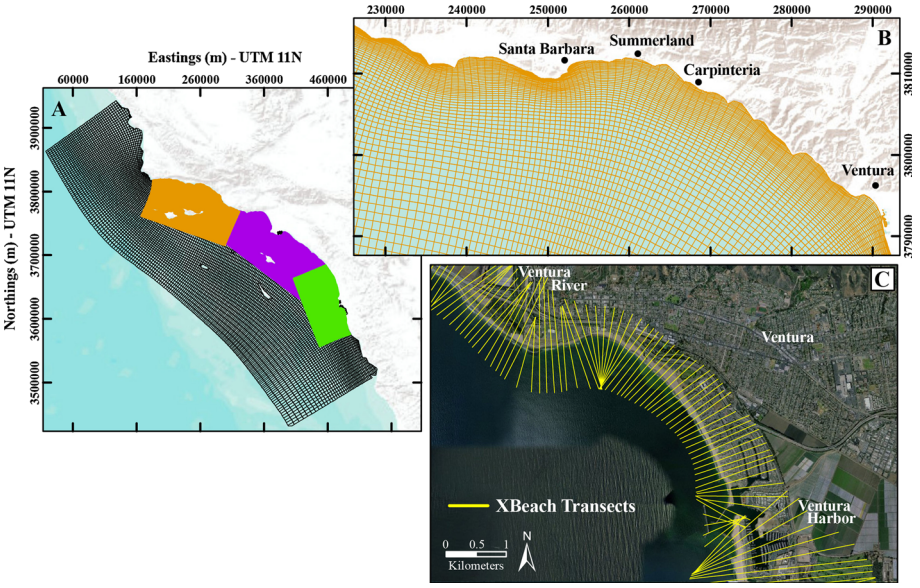

Fig. 6 Nested modeling scheme for Southern California. **a** Overview of Delft3D-FLOW and Delft3D-WAVE models: SoCal (*black*), Santa Barbara Channel (*orange*), Los Angeles/Orange County (*purple*), San Diego (*green*). **b** Detail of the Santa Barbara Channel model. **c** Example of XBeach cross-shore profile model distribution near the city of Ventura (see Fig. 5 for location). (Basemaps from http://services.arcgisonline.com/arcgis/services, World_Terrain_Base and ESRI_Imagery_World_2D, accessed Jan 22, 2014)

and 1986, to simulate a series of storms with a recurrence interval of at least 100 years (Dettinger et al. 2012). The so-called ARkStorm scenario provided a time series of wind and pressure fields that served as boundary conditions for a preliminary evaluation of the CoSMoS model.

The El Niño fueled storm of January 18–25, 2010 produced large waves (max deep water $H_{sig} = 9$ m) that remained elevated for a week, producing some of the most extreme coastal erosion observed for several decades throughout California (Barnard et al. 2011). The recent timing of this event provided numerous observations both for model forcing and validation from a known severe storm and thus served as an optimal extreme storm test case for CoSMoS. In addition to running a hindcast of the January 2010 storm, the same storm-forcing conditions were combined with 2050 and 2100 SLR scenarios of +0.5 and +1.4 m from Rahmstorf (2007). These water levels were added to the tidal forcing for the January 2010 storm to better understand the potential for increased flooding that could result from various SLR scenarios combined with a recent, well-documented coastal storm.

3.3 Storm scenarios—testing and validation

The concurrent development of CoSMoS for both real-time and offline applications provides opportunities to validate model performance in predicting wave heights and water levels in the regional models, because results are continuously compared to wave buoy and tide gauge measurements in the real-time system. Validation of the local models is more

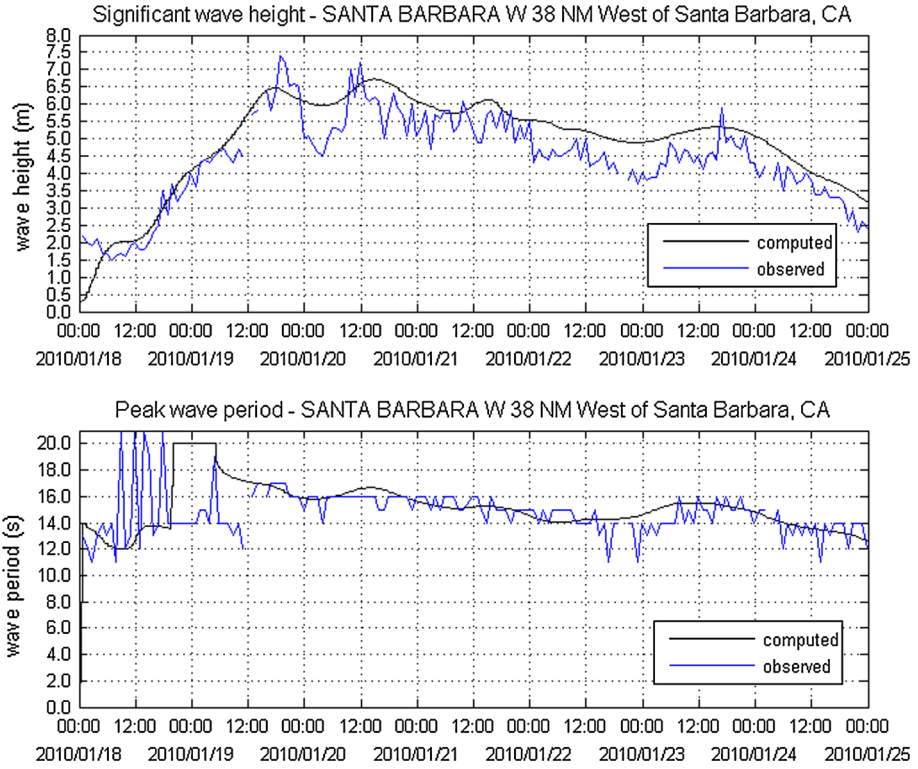

Fig. 7 Deepwater wave model-data comparison from the Harvest Buoy (see Fig. 5 for location) for the January 2010 storm hindcast. Wave data from CDIP (2013)

difficult, as data sets that are ideal for the validation of beach response to storms and run-up are scarce in the project area and the input morphology represents a snapshot in time.

3.3.1 Wave and water levels

The accuracy of modeled wave heights and water levels was investigated in detail for the January 2010 storm and for a longer period (January and February 2011). Figure 7 presents a comparison of the model output to measurements of significant wave height and period from the CDIP Harvest Buoy for the January 2010 storm hindcast. The CDIP Harvest Buoy is located within the Santa Barbara Channel Regional Model (see Figs. 5, 6) in approximately 550 m of water depth. A comparison of modeled and measured water level and nontidal residuals (NTRs) for the tide gauge located on Scripps Pier in La Jolla, CA, shows CoSMoS skill in predicting wave parameters, water levels, and surge for a large storm event (Fig. 8).

For a comparison of hindcasted and observed significant wave heights at CDIP buoys Harvest and Dana Point (see Fig. 5) for January and February 2011, CoSMoS overestimated wave heights at the nearshore and offshore buoys by 12–20 % (Fig. 9). To a large extent, this stems from an overestimation of wave energy in the ENP model. However, on February 9 during one of the largest wave events of the hindcast period, wave heights at the offshore buoys were underestimated by approximately 25 %. At the nearshore buoys, the

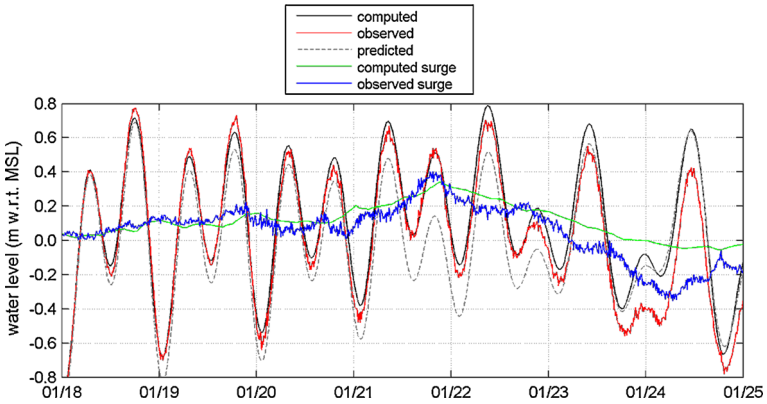

Fig. 8 Nearshore water-level model-data comparison from the La Jolla water-level station (see Fig. 5 for location) for the January 2010 storm hindcast. Water-level data from NOAA (2013c)

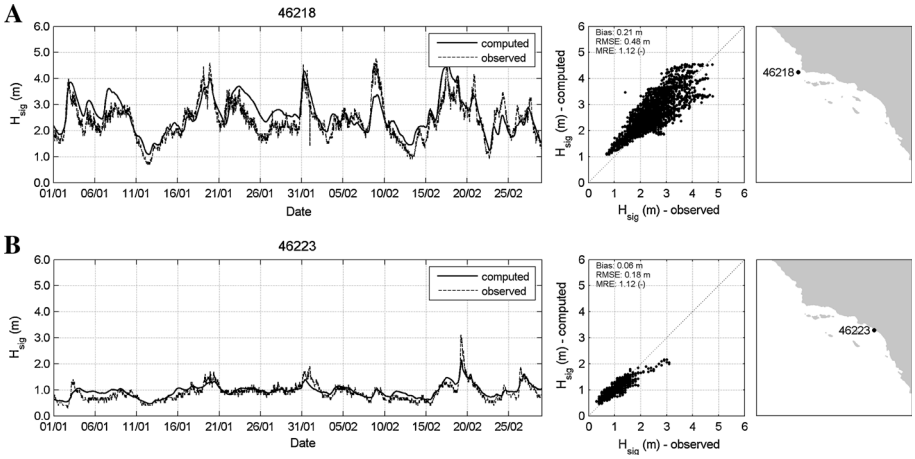

Fig. 9 Comparison of computed and observed wave height at **a** Harvest buoy, and **b** Dana Point buoy. Wave data from CDIP (2013)

model does not capture the peak of locally generated wind waves that occurred on February 19. It is believed that both the temporal (3 hourly) and spatial (12 km) resolutions of the applied NAM wind fields are insufficient to predict this event precisely in the models. In general, the timing of the storm peaks is captured well by the models throughout the hindcast period.

A tidal analysis has been carried out of modeled water levels at a number of tide gauges over a 1-year period (Fig. 10). The model results show a slight overestimation of the semidiurnal components (up to 2 %) and a small underestimation of the diurnal components. The phases of the main tidal constituents are predicted well by the model. Some of the smaller observed components, the largest of which are J1 and NU2, are not included in the model boundary conditions. The total sum of the amplitudes not taken into account in the models is approximately 10 cm. The CoSMoS system presently does not take into account sea-level anomalies due to ocean density gradients, such as those that occur during

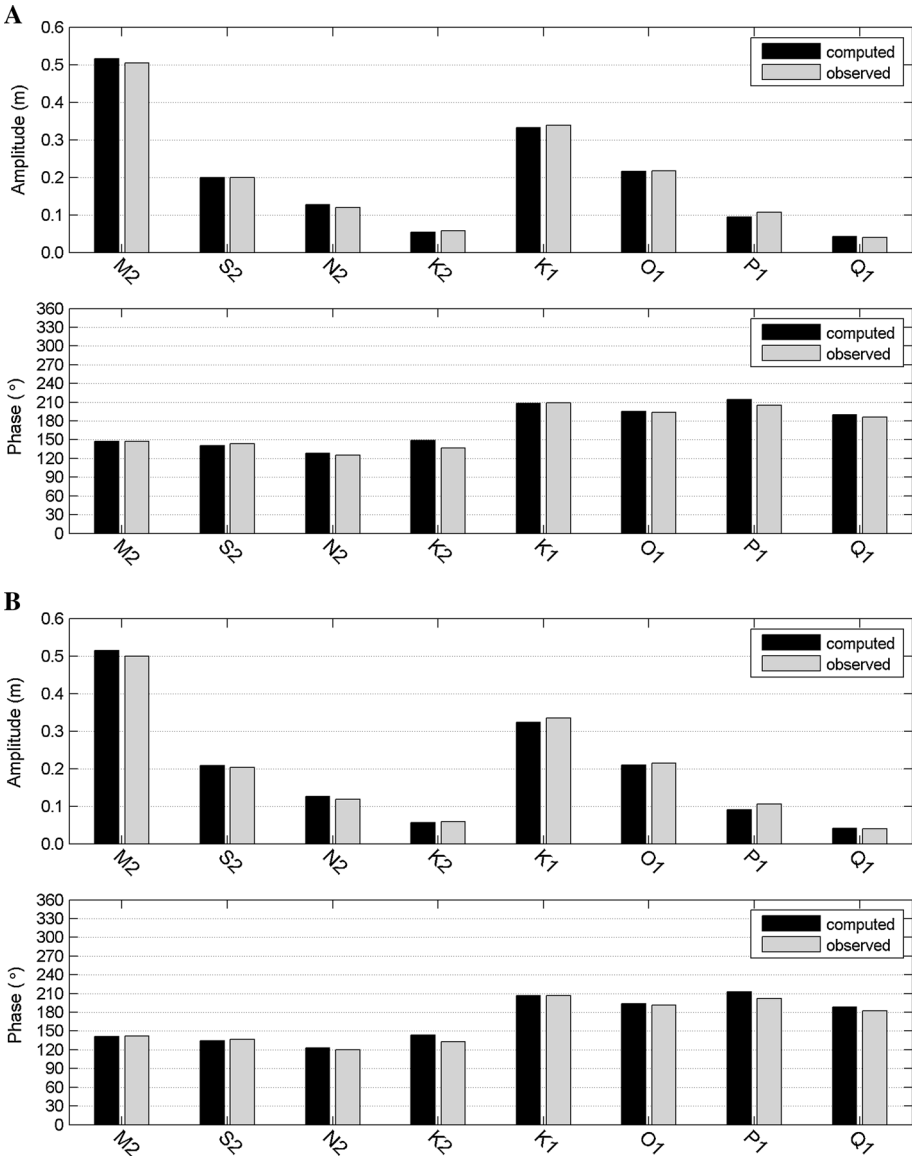

Fig. 10 Comparison of computed and observed tidal constituents at **a** La Jolla, and **b** Santa Monica (see Fig. 5 for locations). Observed tidal constituents obtained from NOAA (2013c)

El Niño events. These would require a 3D modeling approach and accurate boundary conditions for salinity, temperature, and sea surface height.

3.3.2 Cross-shore profile evolution

There are very few data sets collected within the project study area with pre- and post-storm survey data. Scripps Institute of Oceanography (SIO) collected a storm response

Table 3 Skill and bias of XBeach to predict cross-shore profile evolution at Torrey Pines (measured data provided by SIO)

Nearest XBeach station	Skill	Bias (m)
576	0.57	−0.18
581	0.51	−0.25
585	0.64	−0.18
587	0.69	−0.07
594	0.58	+0.06

survey as a component of their project to monitor a beach fill project at Torrey Pines State Beach (Yates et al. 2008), and this data set is the best available for the validation of the profile modeling. The beach and nearshore were surveyed on November 14, 2011 and again on November 28, 2001 following a severe winter storm event with a significant wave height reaching over 3 m (Yates et al. 2008). The XBeach model was applied with the same setup described in Sect. 2.3 along the survey profiles, which are oriented slightly more east–west than the profiles used in the overall CoSMoS system. The entire profile was set to sand since there are not any cliff-backed sections within the survey area. CoSMoS was run with a hindcast of the November 2001 storm to generate forcing for the local model. The XBeach model was forced with bathymetry data from the November 14, 2011 survey (provided by SIO) and water-level and 2D SWAN spectra output from the regional San Diego model (see Fig. 6) at the nearest XBeach model location.

The model skill and bias were calculated for each profile (Table 3) following the methods described in McCall et al. (2010):

$$\text{Skill} = 1 - \frac{\sum_{i=1}^{N}\left(\mathrm{d}z_{b_{\text{meas},i}} - \mathrm{d}z_{b_{\text{xbeach},i}}\right)^2}{\sum_{i=1}^{N}\left(\mathrm{d}z_{b_{\text{meas},i}}\right)^2} \tag{2}$$

$$\text{Bias} = \frac{1}{N}\sum_{i=1}^{N}\left(z_{b_{\text{xbeach},i}} - z_{b_{\text{meas},i}}\right), \tag{3}$$

where N is the number of data points covered by both pre- and post-storm bed-level elevation measurements, $\mathrm{d}z_{b_{\text{meas},i}}$ is the measured bed-level change in point i and $dz_{b_{\text{xbeach},i}}$ is the modeled bed-level change in point i. The skill describes how well the model captures the variance in bed level, and the bias describes the model's overall offset from measurements. Shoreline change statistics were estimated from the XBeach output profiles as a component of the CoSMoS system (Table 4). XBeach generally underestimated the profile erosion on the beach face for this storm event, which leads to some differences in shoreline change estimates (Table 4). The model does show skill in reproducing the general trends of profile evolution; however, it does not reproduce the smaller-scale morphology (multiple bar profile) that was mapped in the measurements, as the model is not capable of reproducing bar migration. Overall, however, the interpretation of the model-data comparison results presented here is limited by the small sample size.

3.3.3 Flood extent Hindcast for January 2005 Newport Harbor flood

One of the difficulties in testing a coastal hazards model is a lack of validation information for the hazards themselves. Flood extents in particular are rarely measured except under the most extreme scenarios (e.g., New Orleans following Hurricane Katrina). Even though

Table 4 Comparison of measured and modeled shoreline change at Torrey Pines (measured data provided by SIO)

Nearest XBeach station	Shoreline change (m)		
	Measured	Modeled	% Diff
576	−26.1	−28.0	+7
581	−36.5	−21.7	−41
585	−34.3	−22.1	−36
587	−32.7	−21.9	−33
594	−15.6	−23.7	+52

waves were not a significant factor, an extreme tide event coupled with an atmospheric low-pressure system caused significant flooding in Newport Harbor (see Fig. 5), on January 10, 2005. The tide was forecast to be 2.19 m above MLLW 8:12 AM LST at the NOAA Los Angeles tide gauge (NOAA 2013c). However, the actual tide measured 2.42, 0.22 m above forecast. Newport Beach officials extensively photo-documented the flooding. Gallien et al. (2011, 2012) georeferenced 85 photographs to delineate the flood extent in ArcGIS. This represents the only known location and event where a coastal flooding event has been quantitatively determined along the entire US West Coast.

CoSMoS was run for this scenario, and the flood hazard map was overlaid with the ground-truthed flood determined from city photographs (Fig. 11). By using wave run-up on the outer coast for a flood that was primarily confined to a protected embayment, CoSMoS conservatively overpredicted the flood extent, but there was a 52 % overlap between CoSMoS predictions and what was measured on the ground, and the spatial coherence of the modeled and observed flood predictions is satisfactory. Gallien et al. (2011; 2012) demonstrate that local flood predictions improve by applying a hydrodynamic model to Newport Harbor and a highly refined local DEM that includes land-based real-time kinematic GPS surveys of important flood protection structures (e.g., 15-cm wide flood walls) that are not resolved by remotely sensed surveys (e.g., Lidar). Nevertheless, given the vast spatial scale CoSMoS covers, the accuracy of the projections for this small area is sufficient and accurate enough to suggest that the modeling system would support effective emergency response planning. In CoSMoS 2.0, all protected embayments are explicitly modeled with high-resolution nested grids to improve water-level predictions in these locations.

3.4 Examples of scenario results

3.4.1 Flooding

Perhaps, the most useful examples of flooding extents predicted by CoSMoS are the progressive flooding caused by the hindcast of the January 2010 storm combined with the additional SLR scenarios of 0.5 and 1.4 m. Over the vast expanse of Southern California, this can clearly identify regions that are vulnerable to coastal flooding now or in the future, and broadly identify water elevation thresholds where SLR tips the balance of coastal vulnerability (Fig. 12). At the local scale, as in the examples from Venice/Marina del Rey and Del Mar (Fig. 13), in addition to the identification of SLR thresholds where flooding vulnerability might become extensive, the pathways for local flooding can also be clearly delineated to guide coastal management planning.

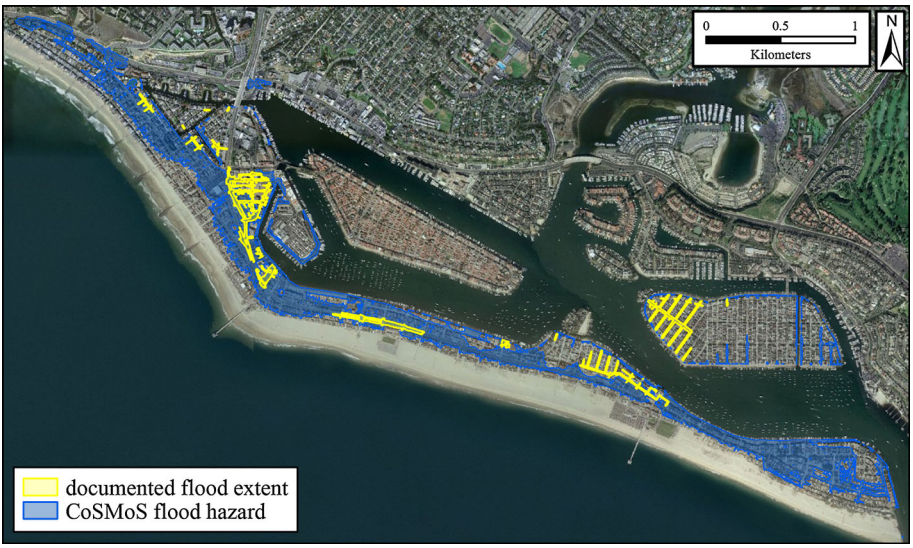

Fig. 11 Flooding projected by CoSMoS versus ground truth (Gallien et al. 2011, 2012) from January 2005 high-tide event in Balboa Harbor, Newport Beach, CA (see Fig. 5 for location). (Basemaps from http://services.arcgisonline.com/arcgis/services, World_Terrain_Base and ESRI_Imagery_World_2D, accessed Jan 22, 2014)

3.4.2 Beach erosion

For each scenario, regional statistics of shoreline change are calculated (Fig. 14) to identify alongshore variability in cross-shore coastal change, in particular areas most vulnerable to erosion within the study area (e.g., Los Angeles County beaches for the ARkStorm scenario). In addition, a vast array of model output (e.g., maximum wave height, maximum run-up, and profile change) is available for each of the 4,723 XBeach transects in Southern California (Fig. 15) to aid local planning. The XBeach profile model results that were located in the vicinity of Torrey Pines were compared with the total envelope of survey data that have been collected at that location by SIO as a component of the Southern California Beach Processes Study (SIO 2009). The survey data at Torrey Pines were gridded, and bathymetry was extracted along the XBeach profiles for comparison to the results of the ARkStorm scenario (Fig. 16). These results show that the modeled volume of profile change resulting from that scenario falls within the normal variation in beach and nearshore elevation at this location. The full scenario results are available in a flexible Google Earth interface covering the entire study area (Fig. 17) and can be downloaded from http://walrus.wr.usgs.gov/coastal_processes/cosmos/socal1.0/index.html).

3.4.3 Cliff failures

Previous probabilistic analyses along the same section of coastline (Hapke and Plant 2010) as assessed for this study indicate that a Bayesian model is well suited to predict coastal cliff retreat over short time periods and that it performs well in identifying sites that are

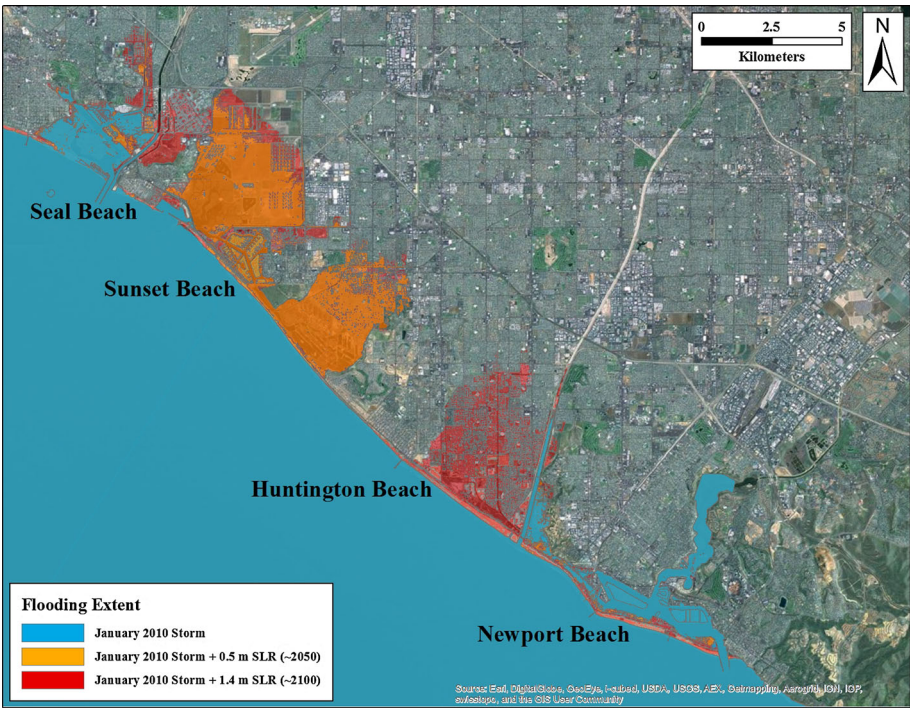

Fig. 12 Flooding projected along the northwestern section of the Orange County coastline (see Fig. 5 for regional location) for the January 2010 storm and the SLR scenarios. (Basemaps from http://services.arcgisonline.com/arcgis/services, World_Terrain_Base and ESRI_Imagery_World_2D, accessed Jan 22, 2014)

most likely to experience high rates of retreat. Hapke and Plant (2010) found that a cross-validation of the Bayesian model output with observed cliff retreat had 89 % accuracy. We assume that the accuracy of results presented here for the ARkStorm scenarios is similar. The uncertainties in the predictions were high for 28 % of the transects, wherein the most probable outcome was equally likely for 3 or more bins. This is the same uncertainty percentage reported for the previous study.

The results indicate that along 56 % of the XBeach transects, coastal cliff retreat from the ARkStorm event is high (−0.5 to −1.0 m) or very high (−1.0 to −5.0 m). Very low retreat is predicted for only 6.4 % of the transects, indicating that even though the storm did not produce substantially high total water levels, the probabilities are high that there will be some amount of cliff retreat along the majority of this coastline. A sensitivity analysis of the model indicates that the amount of cliff retreat is most sensitive to cliff slope and historical rates of retreat. The outcome is least sensitive to geology, which is expected given the lack of variation in the geology parameter (only 2 possible bins). The model could likely be refined by incorporating more detailed information about the lithology and material strength. The predicted outcome varies alongshore, and the majority of the predictions are for higher amounts of cliff retreat (Fig. 18). The variation in the cliff retreat along shore is similar to the trends in the long-term shoreline change.

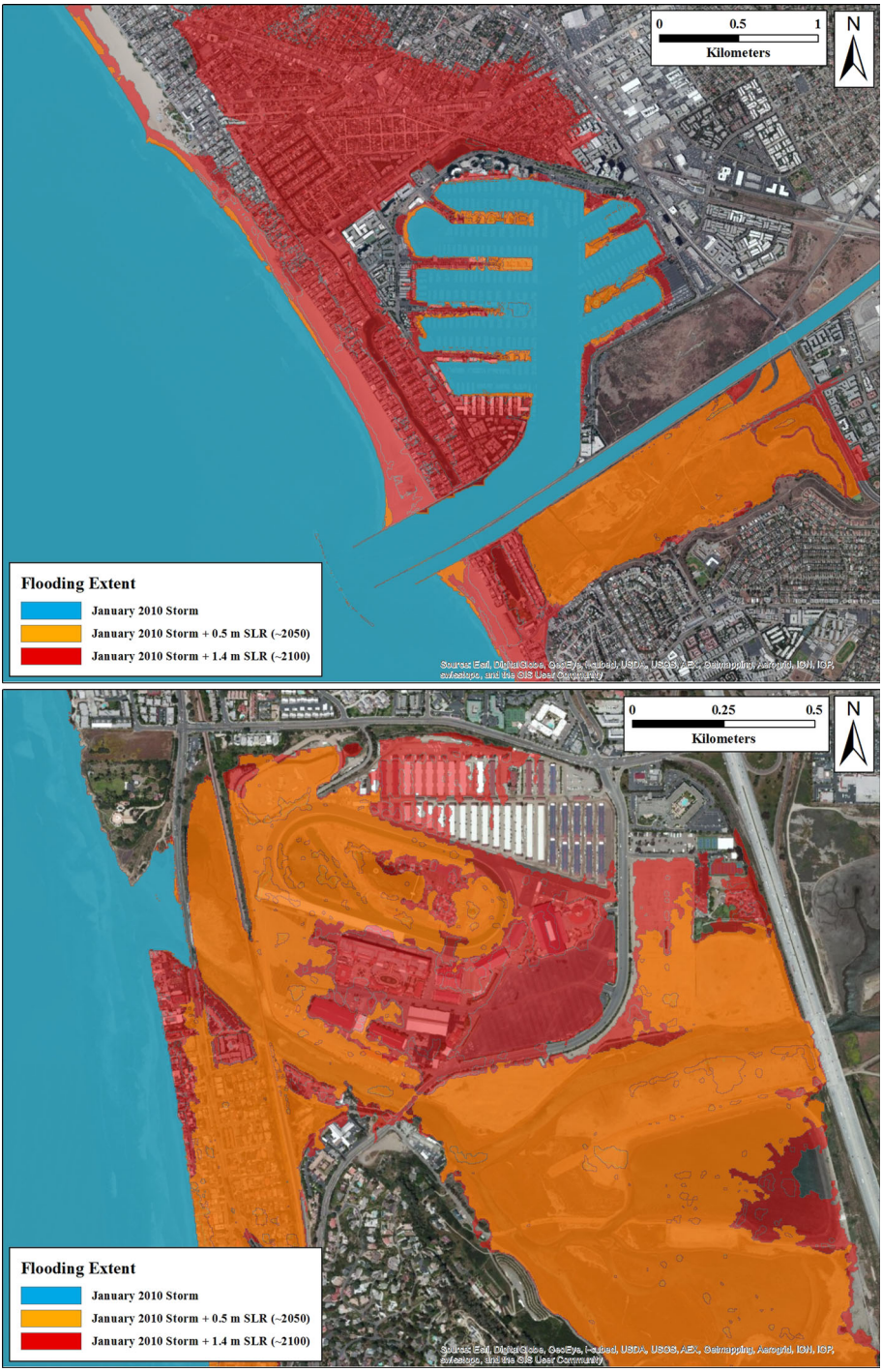
0
0.5
1
Kilometers
N
Flooding Extent
January 2010 Storm
January 2010 Storm + 0.5 m SLR (~2050)
January 2010 Storm + 1.4 m SLR (~2100)
Source: Esri, DigitalGlobe, GeoEye, i-cubed, USDA, USGS, AEX, Getmapping, Aerogrid, IGN, IGP, swisstopo, and the GIS User Community
0
0.25
0.5
Kilometers
N
Flooding Extent
January 2010 Storm
January 2010 Storm + 0.5 m SLR (~2050)
January 2010 Storm + 1.4 m SLR (~2100)
Source: Esri, DigitalGlobe, GeoEye, i-cubed, USDA, USGS, AEX, Getmapping, Aerogrid, IGN, IGP, swisstopo, and the GIS User Community

◀**Fig. 13** Example of flooding hazards predicted from the hindcast of the January 2010 storm and SLR scenarios in the vicinity of Venice/Marina del Rey (*top*) and Del Mar (*bottom*) (see Fig. 5 for locations). (Basemaps from http://services.arcgisonline.com/arcgis/services, World_Terrain_Base and ESRI_Imagery_World_2D, accessed Jan 22, 2014)

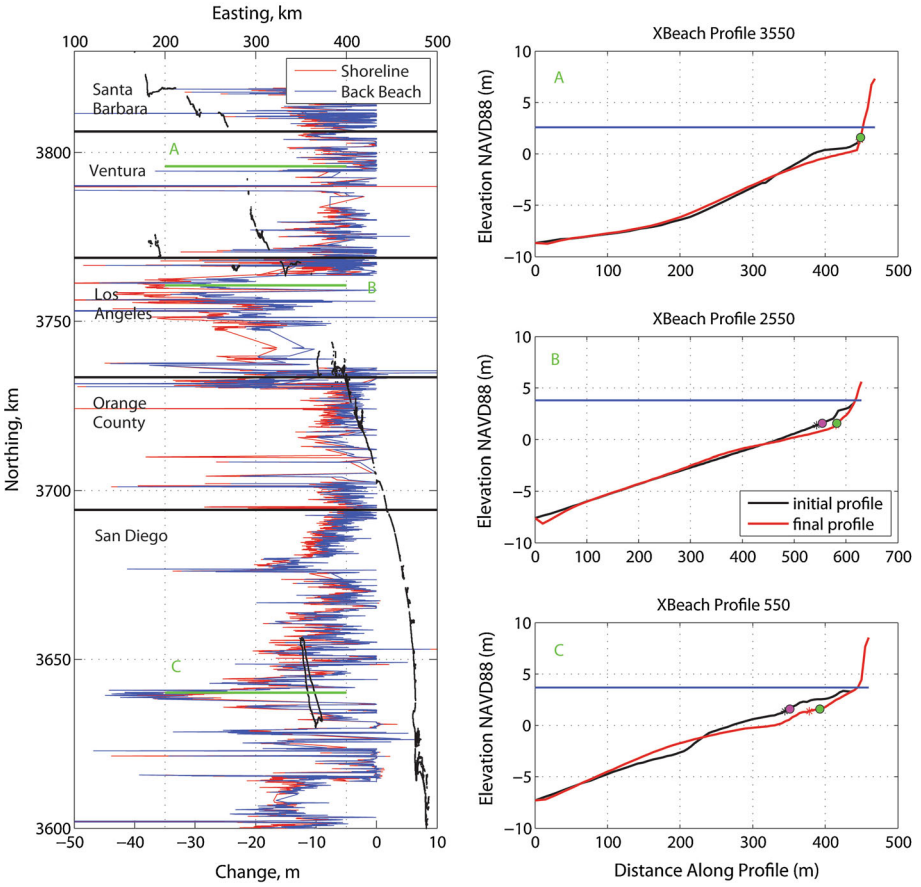

Fig. 14 Predicted shoreline change over the Southern California region based on the ARkStorm Scenario

3.4.4 Erosion hot spots

From the calculation of gradients in longshore sediment transport potential described in Sect. 2.6.2, the CoSMoS modeling system can be used to evaluate and predict locations and magnitudes of erosional hot spots during storms. This technique has been applied to other sites within the Southern California Bight in a previous study (Adams et al. 2011). We conducted such an analysis on the ARkStorm scenario. Figure 19 summarizes the results of an erosional hot spot (EHS) analysis for the period of the storm scenario described above for the Mission Bay Inlet in Southern California (see Fig. 5 for location). The left panel displays the alongshore distribution of nearshore wave height throughout the storm and shows some (minor) alongshore variability in wave height during the storm peak

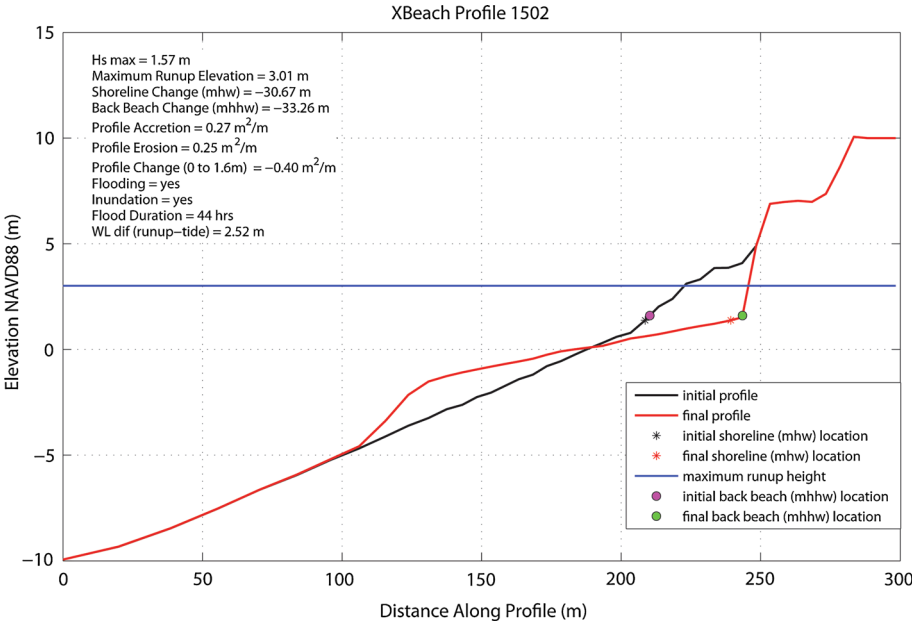

Fig. 15 Example of the detailed parameter predictions for the XBeach model

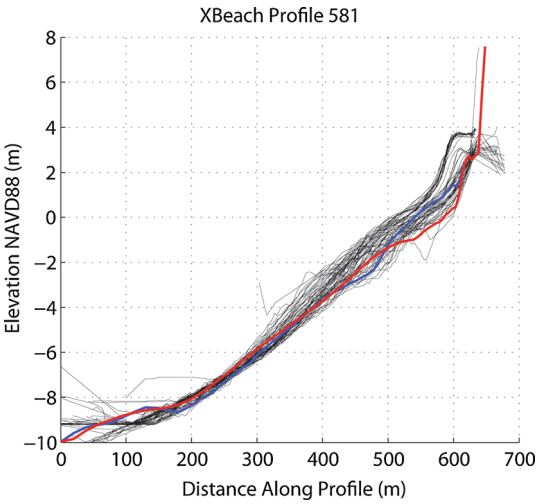

Fig. 16 Comparison of XBeach input (*blue line*) and output (*red line*) to survey envelope (black lines) at XBeach Profile 581 at Torrey Pines (survey envelope data provided by SIO)

at approximately hour 150. The time series of the alongshore distribution of longshore sediment transport (LST) potential, shown in the center panel, illustrates three strong peaked zones in northward (positive) sediment movement, interrupted by zones of dominantly southward transport. The gradients of the LST potential, displayed in the right panel, show several prominent erosional hot spots that persist throughout the duration of the storm south of Mission Bay Inlet, shown by the gap (locations of XBeach Profiles 361–365). Another type of interesting behavior is visible north of the harbor mouth, in the

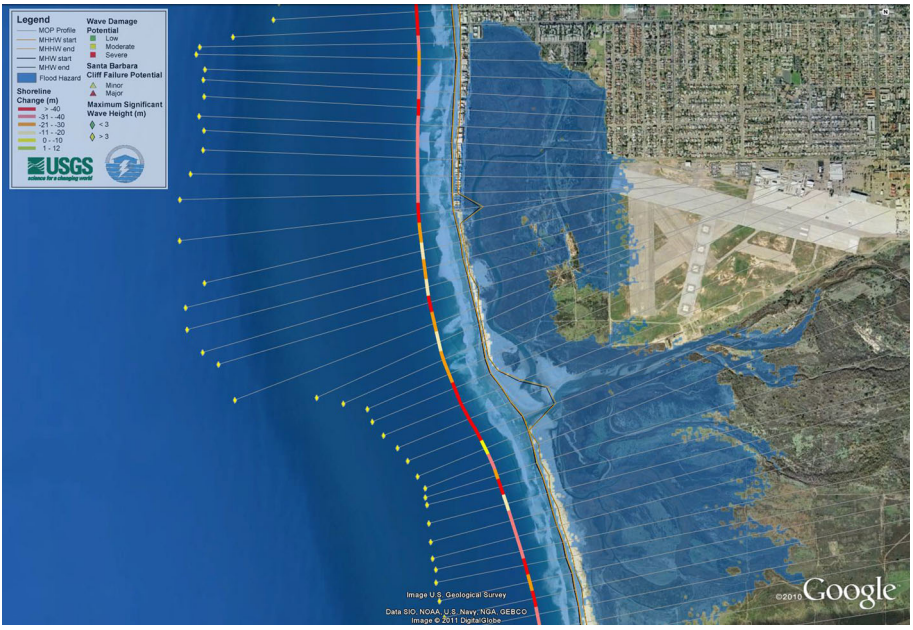

Fig. 17 Flooding and shoreline change projections in the Imperial Beach area of southern San Diego County just north of the Mexican border (see Fig. 5 for location) from the ARkStorm scenario, presented in Google Earth

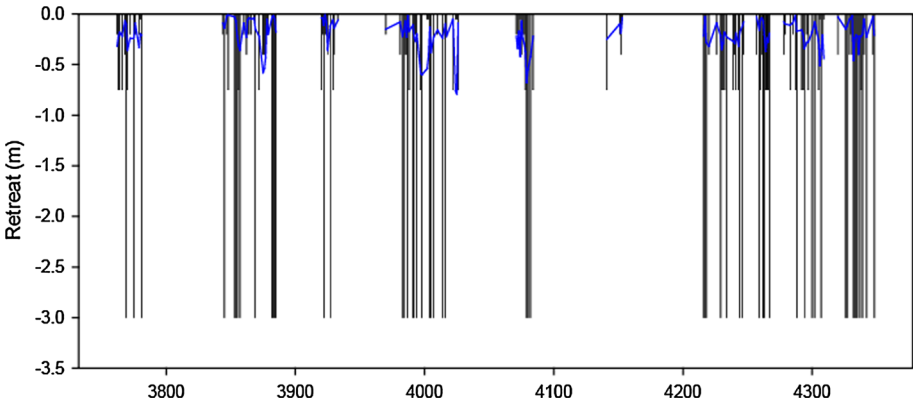

Fig. 18 Coastal cliff retreat prediction results for the ARkStorm scenario in the Santa Barbara Region for XBeach lines 3700–4400. The predicted values of retreat are the center value of each bin. The blue line is the long-term historical rate of change in m/year

vicinity of XBeach transects 365–385. During the waxing limb of the storm, a narrow erosional hot spot migrates rapidly southward alongshore at a rate of approximately 75 m/h, then reverses direction, and migrates northward at approximately the same rate during the waning limb. This behavior is likely due to the interaction of the time-varying wave conditions with a complex bathymetry that strongly influences the refraction patterns. It is

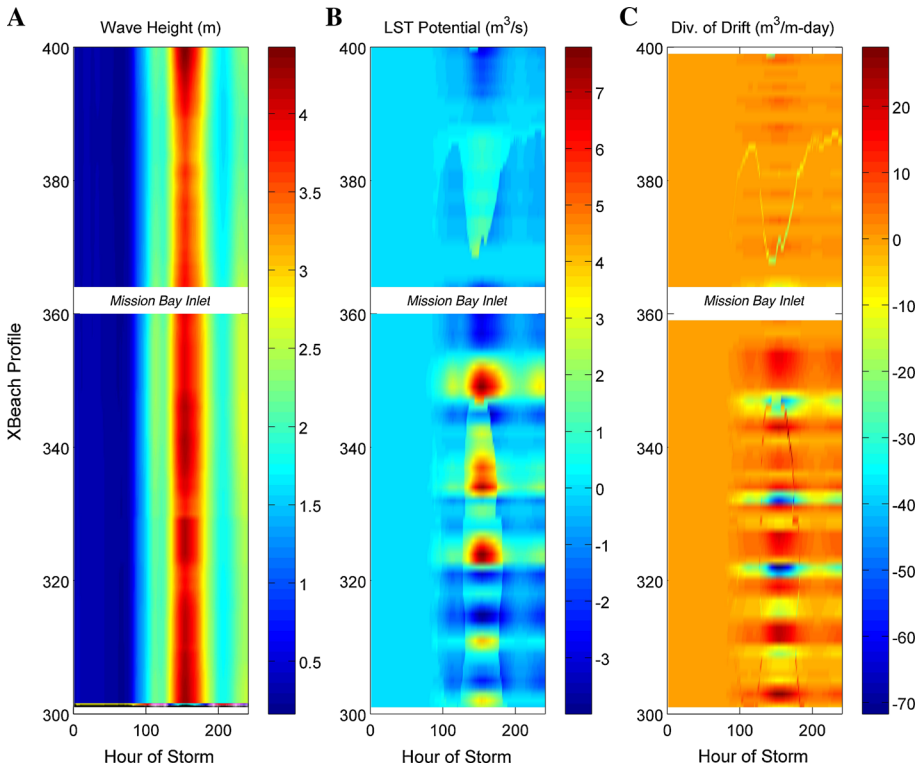

Fig. 19 Results of erosional hot spot analysis conducted for ARkStorm scenario in the Mission Bay region of San Diego (see Fig. 5 for location). **a** Longshore distributions of nearshore wave height, **b** longshore sediment transport rate potential assuming a transport-limited scenario, and **c** volumetric erosion per unit length shoreline, throughout the course of the storm

unlikely that such behavior would be predictable without a multicomponent modeling system such as the one described in this manuscript. For much of the California coast, a supply limited case may be more appropriate.

4 CoSMoS 2.0: case study of future climate scenarios in North-Central California

Future storm conditions are likely to evolve in a fashion that is unlike past conditions and is ultimately dependent on the complicated interaction between the Earth's atmosphere and ocean systems, fueled by climate change. Therefore, the past several decades of wave measurements may not be indicative of the future wave climate (Hemer et al. 2013). In order to perform a robust climate impacts assessment of the 170-km long, North-Central California coast, a twenty-first century wave climatology was first established using the wind fields from CMIP5 (2011) GCMs. The wind fields from the RCP 4.5 and 8.5 scenarios for 4 GCMs with sufficient temporal resolution to resolve peak conditions (3 h) were fed into the WAVEWATCH III wave models within CoSMoS and dynamically downscaled to develop an ensemble wave climatology for the US West Coast through 2100. From that established wave climatology, standard return level events (e.g., mean,

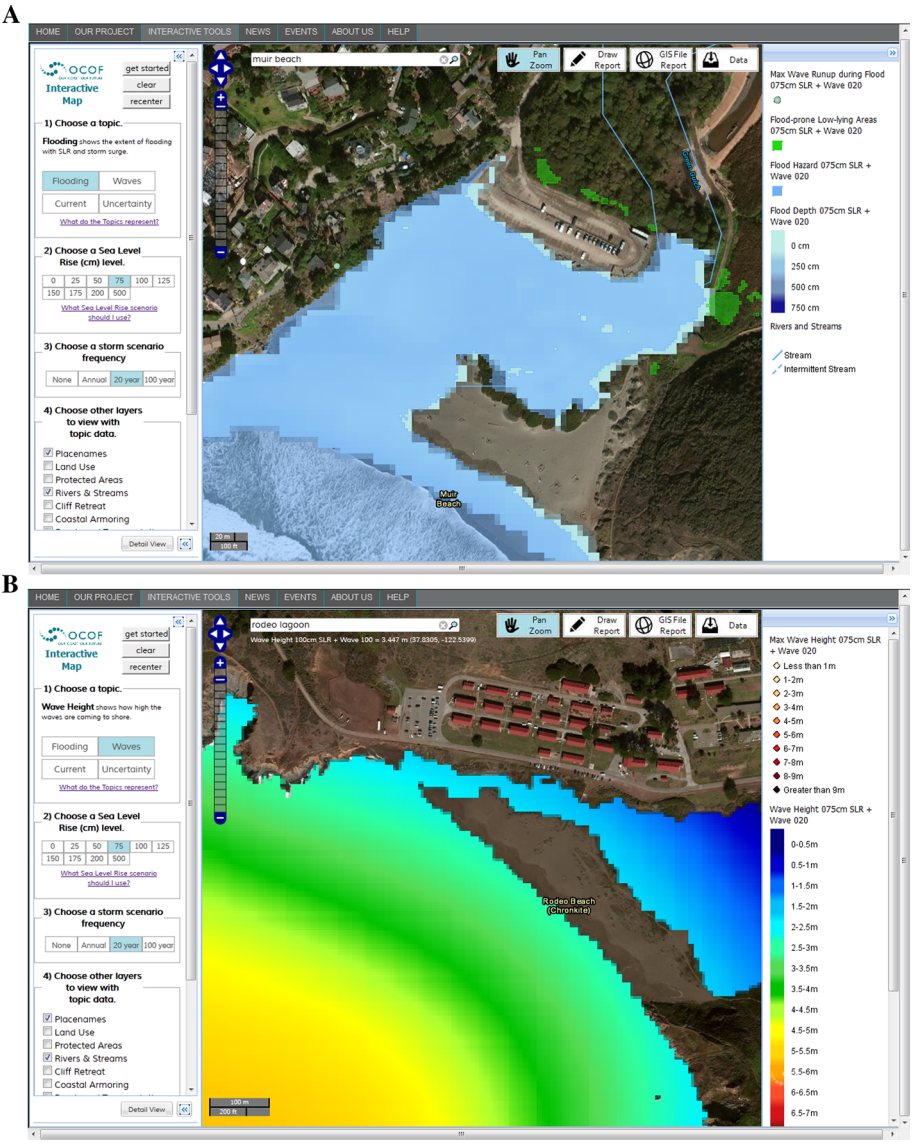

Fig. 20 Example screenshots of the Web tool developed to serve up CoSMoS 2.0 model output along the North-central California coast as part of the Our Coast-Our Future project (www.prbo.org/ocof): **a** flooding for Muir Beach, and **b** wave height adjacent to Rodeo Beach, two sites immediately north of the city of San Francisco

annual, 20 years, and 100 years) were extracted to serve as boundary conditions for CoSMoS simulations in the study area. Those wave events were combined with the full spectrum of plausible twenty-first century SLR (0–2 m in 25 cm increments) along with an extreme 5 m SLR (Hansen 2007) for a total of 40 combinations of wave conditions and SLR. Those offshore wave conditions, with regional additions of wind, atmospheric

pressure, tides, and SLR, were modeled down to the local scale to produce hazard projections using the standard CoSMoS framework and product line (see Fig. 1). Further details of this approach will be provided in a future publication, as well as for a similar effort in San Francisco Bay.

In addition to a robust technique for establishing the future wave climatology, CoSMoS 2.0 also features the addition of a sophisticated Web tool (www.prbo.org/ocof). It allows the user to select from each of the 40 combinations of SLR and storms to visualize the flooding depth, extent, and uncertainty associated with each event, in addition to the predictions of wave heights, current strength, and event-based shoreline change. The results are overlain with an extensive database of ecology, land use, and infrastructure attributes (Fig. 20).

5 Discussion and conclusions

The Coastal Storm Modeling System (CoSMoS) is a multidimensional, deterministic modeling system that can scale down from global atmospheric forcing to local hazards assessments. In examples from the California coast, this modeling approach has been shown to adequately predict waves, water levels, coastal flooding, and coastal change over vast geographic regions with resolution and accuracy fine enough to aid local coastal management planning in real time or for future climate change impacts.

A current limitation of CoSMoS is the use of a static DEM for flooding projections. A warming climate has the potential to not only raise sea level but also to exacerbate coastal change hazards due to alterations in ocean circulation patterns, tidal amplitudes, winds, and storms (Ruggiero 2008; Ruggiero et al. 2010). These potentially changing factors all contribute to uncertainties in future shoreline positions, and therefore, a complete hazards assessment should include sophisticated and accurate predictions of coastal change (beaches and cliffs) associated with climate change over the next century. Any approach should consider dynamic feedbacks between the cliff and beach, alongshore and cross-shore heterogeneity in substrate composition, and coupled feedback with physical process modeling. We are currently developing a methodology to make long-term coastal change projections as part of a complementary module within CoSMoS that will then feed back into a dynamic DEM to enable more precise projections of future flooding extents based upon a temporally evolving coastline.

Additionally, the seas and setup fueled by local winds, particularly in large, protected embayments such as San Francisco Bay where swell is not dominant, can exert a significant influence on coastal flooding extents and geomorphic change. Where local wind-driven processes are not adequately resolved by the coarse resolution of GCMs, statistically or dynamically downscaled winds may greatly improve hazards assessments.

Although current limitations exist, CoSMoS can provide reasonably accurate projections to aid emergency response managers and coastal planners over large geographic regions in identifying local sites with notable storm and/or SLR vulnerabilities. Despite a lack of available data and tools to address future impacts, consideration of climate change is increasingly becoming a requirement for any entity with coastal jurisdiction. Here, we have presented a robust modeling approach to meet that need.

Acknowledgments The authors wish to thank the US Geological Survey, Deltares, NOAA, and the National Park Service for funding this research. Early peer reviews of CoSMoS were provided by Jim Bailard, Rebecca Beavers, Carolynn Box, Kate Dallas, Lesley Ewing, Doug George, Bob Guza, Dan Hanes,

Jeff Hansen, Dan Hoover, Jeff List, Bill O'Reilly, Dano Roelvink, Julie Thomas, and Dirk-Jan Walstra. PNA thanks Jessica Lovering for assistance with LST gradient calculations. Torrey Pines beach survey data and concurrent nearshore wave predictions were provided by Scripps Institution of Oceanography and were funded by the California Department of Parks and Recreation, Division of Boating and Waterways, and the US Army Corps of Engineers. The most up-to-date information on CoSMoS, including study areas, methods, model results, and publications, can be found at http://walrus.wr.usgs.gov/coastal_processes/cosmos/index.html.

References

Adams PN, Inman D, Graham N (2008) Southern California deep-water wave climate: characterization and application to coastal processes. J Coast Res 24(4):1022–1035

Adams PN, Inman DL, Lovering JL (2011) Effects of climate change and wave direction on longshore sediment transport patterns in Southern California. Clim Change 109(S1):211–228. doi:10.1007/s10584-011-0317-0

Allan JC, Komar PD (2006) Climate controls on US West Coast erosion processes. J Coast Res 22(3):511–529

Allan JC, Komar PD, Ruggiero P (2011) Storm surge magnitude and frequency on the central Oregon coast. Proceedings of the solutions to coastal disasters conference 2011, 13 p

Barnard PL, Hoover D (2010) A seamless, high-resolution, coastal digital elevation model (DEM) for Southern California. U.S. Geological Survey Data Series 487: 8 p. http://pubs.usgs.gov/ds/487/

Barnard PL, O'Reilly B, van Ormondt M, Elias E, Ruggiero P, Erikson LH, Hapke C, Collins BD, Guza RT, Adams PN, Thomas JT (2009) The framework of a coastal hazards model: a tool for predicting the impact of severe storms. U.S. Geological Survey Open-File Report 2009–1073:19 p. http://pubs.usgs.gov/of/2009/1073/

Barnard PL, Allan J, Hansen JE, Kaminsky GM, Ruggiero P, Doria A (2011) The impact of the 2009-10 El Niño Modoki on U.S. West Coast beaches. Geophys Res Lett 38 (L13604):7

Bender MA, Ginis I (2000) Real-case simulations of hurricane–ocean interaction using a high-resolution coupled model: effects on hurricane intensity. Mon Weather Rev 128:917–946

Bender MA, Ginis I, Tuleya R, Thomas B, Marchok T (2007) The operational GFDL coupled hurricane–ocean prediction system and a summary of its performance. Mon Weather Rev 135:3965–3989

Bromirski PD, Flick RE, Cayan DR (2003) Storminess variability along the California coast: 1858–2000. J Clim 16(6):982–993

Cayan DR, Bromirski PD, Hayhoe K, Tyree M, Dettinger MD, Flick RE (2008) Climate change projections of sea level extremes along the California coast. Clim Change 87(Suppl. 1):S57–S73

Chen SS, Price JF, Zhao W, Donelan MA, Walsh EJ (2007) The CBLAST Hurricane program and the next-generation fully coupled atmosphere–wave–ocean models for hurricane research and prediction. Bull Am Meteorolog Soc 88:311–317

Coastal Data Information Program (CDIP) (2013) Scripps Institution of Oceanography, Integrative Oceanography Division, San Diego, http://cdip.ucsd.edu

Coastal Engineering Research Center (CERC) (1984) Shore Protection Manual. U.S. Army Corps of Engineers, Coastal Engineering Research Center. U.S. Government Printing Office, Washington

Coupled Model Intercomparison Project, Phase 5 (CMIP5) (2011) WCRP Coupled Model Intercomparison Project—Phase 5. Special Issue of the CLIVAR Exchanges Newslett 56 15(2): 52

Delft Hydraulics (2007) User manual Delft3D-FLOW. WL/Delft Hydraulics, Delft, p 614

Dettinger MD, Ralph FM, Hughes M, Das T, Neiman P, Cox D, Estes G, Reynolds D, Hartman R, Cayan D, Jones L (2012) Design and quantification of an extreme winter storm scenario for emergency preparedness and planning exercises in California. Nat Hazards 60:1085–1111. doi:10.1007/s11069-011-9894-5

Egbert G, Bennett A, Foreman M (1994) TOPEX/Poseidon tides estimated using a global inverse model. J Geophys Res 99(C12):24821–24852

Elias EPL, Hansen JE (2013) Understanding processes controlling sediment transports at the mouth of a high-energetic inlet system (San Francisco Bay, CA). Mar Geol 345:207–220. doi:10.1016/j.margeo.2012.07.003

Federal Emergency Management Agency (FEMA) (2007) Coastal Hazards Analysis Modeling Program Version 2.0, User Manual: 50 p

Foxgrover AC, Barnard PL (2012) A seamless, high-resolution digital elevation model (DEM) of the North-Central California coast. U.S. Geological Survey Data Series 684:11. http://pubs.usgs.gov/ds/684/

Gallien TW, Schubert JE, Sanders BF (2011) Predicting tidal flooding of urbanized embayments: a modeling framework and data requirements. Coast Eng 58:567–577

Gallien TW, Barnard PL, van Ormondt M, Foxgrover AC, Sanders BF (2012) A parcel-scale coastal flood forecasting prototype for a Southern California urbanized embayment. J Coast Res 29(3):642–656. doi:10.2112/JCOASTRES-D-12-00114.1

Gemmrich J, Thomas B, Bouchard R (2011) Observational changes and trends in northeast Pacific wave records. Geophys Res Lett 38(L22601):5. doi:10.1029/2011GL049518

Guza RT, Thornton EB (1981) Wave set-up on a natural beach. J Geophys Res 86(C5):4133–4137

Hansen JE (2007) Scientific reticence and sea level rise. Environ Res Lett 2(024002):7. doi:10.1088/1748-9326/2/2/024002

Hapke C, Plant N (2010) Predicting coastal cliff erosion using a Bayesian probabilistic model. Mar Geol 278:140–149. doi:10.1016/j.margeo.2010.10.001

Hapke CJ, Reid D (2007) The National assessment of shoreline change: Part 4, historical coastal cliff retreat along the California coast. U.S. Geological Survey Open-file Report 2007–1133. http://pubs.usgs.gov/of/2007/1133/

Hemer MA, Fan Y, Mori N, Semedo A, Wang XL (2013) Projected changes in wave climate from a multi-model ensemble. Nat Clim Change 3:471–476. doi:10.1038/nclimate1791

Hinkel J, Nicholls RJ, Tol RSJ, Wang ZB, Hamilton JM, Boot G, Vafeidis AT, McFadden L, Ganopolski A, Klein RJT (2013) A global analysis of erosion of sandy beaches and sea-level rise: an application of DIVA. Glob Planet Change 111:150–158

Komar PD, Inman DL (1970) Longshore sand transport on beaches. J Geophys Res 75(30):5914–5927

Lesser GR, Roelvink JA, van Kester JA, Stelling GS (2004) Development and validation of a three-dimensional morphological model. Coast Eng 51:883–915

McCall RT, Thiel Van, de Vries JSM, Plant NG, Van Dongeren AR, Roelvink JA, Thompson DM, Reniers AJHM (2010) Two-dimensional time dependent hurricane overwash and erosion modeling at Santa Rosa Island. Coast Eng 57:668–683. doi:10.1016/j.coastaleng.2010.02.006

Menendez M, Mendez FJ, Losada IJ, Graham NE (2008) Variability of extreme wave heights in the northeast Pacific Ocean based on buoy measurements. Geophys Res Lett 35(L22607):6. doi:10.1029/2008GL035394

Minor SA, Kellogg KS, Stanley RG, Stone P, Powell II CL, Gurrola LD, Selting AJ, Brandt TR (2002) Preliminary geologic map of the Santa Barbara Coastal Plain Area, Santa Barbara County, California. U.S. Geological Survey Open-file Report 02–136. http://pubs.usgs.gov/of/2002/ofr-02-0136/

National Oceanic and Atmospheric Administration (NOAA) (2011) WaveWatch III Model. Center of Operational Products and Services. http://polar.ncep.noaa.gov/waves/wavewatch/wavewatch.html. Accessed 15 Aug 2011

National Oceanic and Atmospheric Administration (NOAA) (2013a) National Data Buoy Center. http://www.ndbc.noaa.gov/. Accessed 10 Dec 2013

National Oceanic and Atmospheric Administration (NOAA) (2013b) Sea level rise and coastal flooding impacts viewer. Coastal Services Center. http://www.csc.noaa.gov/slr/viewer/#. Accessed 10 Dec 2013

National Oceanic and Atmospheric Administration (NOAA) (2013c) Tides & Currents. Center for Operational Products and Services. http://tidesandcurrents.noaa.gov/. Accessed 10 Dec 2013

National Research Council (2012) Sea-level rise for the coasts of California, Oregon, and Washington: past, present, and future. Committee on Sea Level Rise in California, Oregon, and Washington. The National Academies Press, Washington, 260 p

National Weather Service (NWS) (2012) California's Top 15 weather events of 1900's. National Oceanic and Atmospheric Administration. http://www.wrh.noaa.gov/pqr/paststorms/california10.php#1982-83%20El%20Nino%20Storms. Accessed 9 November 2012

National Weather Service (NWS) (2013) Climate prediction. National Oceanic and Atmospheric Administration. http://www.nws.noaa.gov/predictions.php Accessed 10 December 2013

Nicholls RJ (2004) Coastal flooding and wetland loss in the 21st century: changes under the SRES climate and socio-economic scenarios. Glob Environ Change 14:69–86. doi:10.1016/j.gloenvcha.2003.10.007

O'Reilly W (1993) The southern California wave climate–effects of islands and bathymetry. Shore Beach 61(3):14–19

O'Reilly WC, Guza RT (1993) A comparison of spectral wave models in the Southern California Bight. Coast Eng 19(3):263–282

O'Reilly WC, Seymour RJ, Guza RT, Castel D (1993) Wave monitoring in the Southern California Bight. Ocean Wave Measurement and Analysis. Proceedings of 2nd International Symposium, pp 849–863

Pfeffer WT, Harper JT, O'Neel S (2008) Kinematic constraints on glacier contributions to 21st-century sea-level rise. Science 331:1340–1343

Rahmstorf S (2007) A semi-empirical approach to projecting future sea level rise. Science 315:368–370. doi:10.1126/science.1135456
Roelvink D, Reniers A, Van Dongeren A, van Thiel de Vries J, Lescinski J, McCall R (2008) Modeling hurricane impacts on beaches, dunes, and barrier islands. In Smith JM (ed) Coastal Engineering 2008, Proceedings of the 31st International Conference vol 5, 14 p
Roelvink D, Reniers A, Van Dongeren A, van Thiel de Vries J, McCall R, Lescinski J (2009) Modelling storm impacts on beaches, dunes and barrier islands. Coast Eng 56(11–12):1133–1152
Ruggiero P (2008) Impacts of climate change on coastal erosion and flood probability in the US Pacific Northwest. Proceedings of Solutions to Coastal Disasters 2008: 12 p
Ruggiero P (2013) Is the intensifying wave climate of the U.S. Pacific Northwest increasing flooding and erosion risk faster than sea-level rise? J Port Waterw Eng 139(2):88–97
Ruggiero P, Komar PD, Allan JC (2010) Increasing wave heights and extreme-value projections: the wave climate of the U.S., Pacific Northwest. Coast Eng 57:539–552. doi:10.1016/j.coastaleng.2009.12.005
Santoso A, McGregor S, Jin F, Cai W, England MH, An S, McPhaden MJ, Guilyardi E (2013) Late-twentieth-century emergence of the El Niño propagation asymmetry and future projections. Nature 504:126–130. doi:10.1038/nature12683
Scripps Institution of Oceanography (SIO) (2009) Southern California beach processes study survey archive. http://cdip.ucsd.edu/SCBPS/?nav=data. Accessed 12 Oct 2009
Shepard FP (1950) Beach cycles in Southern California. Memo 20, Beach Erosion Board, U.S. Army Corps of Engineers, Washington, 26 p
Splinter KD, Palmsten ML (2012) Modeling dune response to an East Coast Low. Mar Geol 329–331:46–57
Stockdon H, Holman R, Howd P, Sallenger AH (2006) Empirical parameterization of setup, swash, and runup. Coast Eng 53:573–588
Tolman HL (1997) User manual and system documentation of WAVEWATCH-III version 1.15. NOAA/NWS/NCEP/OMB Technical Note 151:97 pp
Tolman HL (2009) User manual and system documentation of WAVEWATCH III version 3.14. NOAA/NWS/NCEP/MMAB Technical Note 276:194 p
Van Dongeren A, Bolle A, Vousdoukas I, Plomaritis T, Eftimova P, Williams J, Armaroli C, Idier D, Van Geer P, Van Thiel de Vries J, Haerens P, Taborda R, Benavente J, Trifonaova E, Ciavola P, Balouin Y, Roelvink D (2009) MICORE: Dune erosion and overwash model validation with data from nine European field sites. Proceedings of Coastal Dynamics 2009, Paper No. 82
Verboom GK, Slob A (1984) Weakly-reflective boundary conditions for two-dimensional water flow problems. Adv Water Resour 7(4):192–197
Vermeer M, Rahmstorf S (2009) Global sea level linked to global temperature. Proc Natl Acad Sci 106(51):21527–21532
Warner JC, Armstrong B, He R, Zambon JB (2010) Development of a Coupled Ocean–Atmosphere–Wave–Sediment Transport (COAWST) modeling system. Ocean Model 35(3):230–244
Yates ML, Guza RT, O'Reilly WC, Seymour RJ (2008) Seasonal persistence of a small Southern California beach fill. Coast Eng 56:559–564. doi:10.1016/j.coastaleng.2008.11.004i
Young IR, Zieger S, Babanin AV (2011) Global trends in wind speed and wave height. Science 332:451–455